

1 Isotopic variations in surface waters and groundwaters of an extremely arid
2 basin and their responses to climate change ~~Spatial-Seasonal Isotopic Variations in~~
3 ~~a Surface-Groundwater System in an Extremely Arid Basin and the Associated~~
4 Hydrogeological Indications

5 Yu Zhang¹, Hongbing Tan^{1,*}, Peixin Cong¹, Dongping Shi¹, Wenbo Rao¹, Xiyong Zhang²

6 ¹School of Earth Sciences and Engineering, Hohai University, Nanjing 210098, China

7 ²Qinghai Institute of Salt Lakes, CAS, Xining 810008, China

8 * **Corresponding author:** Hongbing Tan (tan815@sina.com)

9 **Abstract**

10 Climate changewarming accelerates the global water cycle. However, the relationships
11 between climate changewarming and hydrological processes in the alpine arid regions remain
12 elusiveunclear. ~~Herein, We sampled surface water and groundwater at high spatial and temporal~~
13 ~~spatiotemporal-resolution sampling of surface water and groundwater was performed at to~~
14 investigate these relationships in the Qaidam Basin, an extremely arid area in the northeastern
15 Tibetan Plateau. Stable H-O isotopes and radioactive ³H isotopes were combined with atmospheric
16 simulations to examine hydrological processes and their response mechanisms to climate
17 changeclimate change and hydrogeological characteristics. Contemporary climate processesrules
18 and change dominate the spatial and temporal variations distribution-pattern-of surface water
19 isotopes, specifically, the westerlies moisture transportation intensitywesterly water vapor
20 transport intensity and the local temperature and precipitation regimes. ~~The surface water heavy~~
21 ~~isotopes enrich during the wet season and deplete during the dry season~~. The spatial H-O isotopic
22 compositions in the Eastern Kunlun Mountains showed a gradually depleted eastward pattern;
23 while a reverse pattern occurred in the Qilian Mountains water system. ~~The~~ Precipitation
24 contribution-contributed significantly more to of precipitation to river discharge was considerably
25 higher in the eastern region-of-the basin (approximately 45%) than in the entral-middle and
26 western basinregions (10%–15%). ~~The H-O isotopic compositions showed a gradually negative~~
27 ~~spatial pattern from the west to the east in the Eastern Kunlun Mountains water system; a reverse~~
28 ~~pattern occurred in the Qilian Mountains water system~~. ~~This distribution pattern was jointly~~
29 ~~regulated by the westerly water vapor transport intensity and local hydrothermal condition~~.

30 ~~Moreover, increased~~ increasing precipitation and ~~shrinking cryosphere~~ cryosphere ~~shrinkage~~
31 caused by ~~current~~ climate ~~warming change~~ have ~~mainly~~ accelerated basin groundwater
32 ~~circulation~~ cycle. In the eastern and southwestern Qaidam Basin, precipitation and ~~ice/snow~~
33 meltwater infiltrate ~~along preferential flow paths~~ structural channels that favor water flow, such as
34 ~~fractures~~ faults, ~~volcanic channels~~, and fissures, ~~permitting~~ facilitating rapid seasonal groundwater
35 recharge and ~~enhanced~~ increased terrestrial water storage. However, ~~compensating for water loss~~
36 ~~due to long-term ice and snow melt will be a challenge~~ under ~~projected~~ future increases in increasing
37 precipitation in the southwestern Qaidam Basin, ~~compensating for water loss from long-term~~
38 ~~melting of ice and snow will be challenging~~, and the total water ~~storage~~ resources may show ~~an a~~
39 ~~trend of initially~~ increasing and ~~then before~~ decreasing ~~trend~~. ~~Great uncertainty about water is a~~
40 ~~potential climate change risk facing the arid Qaidam Basin.~~

41 **Keywords:** ~~Qaidam Basin; isotope hydrology; water cycle; spatiotemporal pattern; climate~~

42 1. Introduction

43 ~~In the face of ongoing environmental changes~~ Amidst the impending climate change process,
44 ~~a thorough understanding~~ an in-depth study of the hydrological cycle ~~processes~~ is a prerequisite for
45 ~~accurate trend forecasting, and helps to design efficient water resource management~~
46 ~~strategies~~ implementing water resource management and trend forecasting. Over the past half-
47 century, ~~continuous~~ climate ~~change~~ warming and ~~more intense~~ intensified human activities have led
48 to global water cycle acceleration and water resource redistribution at different scales (Huntington
49 et al., 2006; Durack et al., 2012; Masson-Delmotte et al., 2021). For example, rapid warming has
50 ~~sharply expanded~~ driven the ~~lakes~~ rapid expansion of lakes in the Tibetan Plateau and ~~the shrunk~~
51 ~~them~~ shrinking of lakes in the Mongolian Plateau (Zhang et al., 2017), and ~~it~~ has also
52 ~~exacerbated~~ amplified the severe ~~shortage of~~ irrigation water ~~shortage~~ in parts of South Asia and
53 East Asia (Haddeland et al., 2014). Moreover, ~~it~~ warming is expected to ~~also~~ reduce groundwater
54 storage in the western ~~region of the~~ United States (Condon et al., 2020). ~~Currently~~ At present, the
55 ~~climate in~~ arid regions of northwestern China ~~is changing~~ are undergoing a change in climate from
56 warm-dry to warm-~~humid-wet~~ (Zhang et al., 2021). The resulting uncertainties in ~~water resources~~
57 ~~in arid alpine~~ arid basins ~~water resources in this region present pose~~ new challenges ~~in to~~
58 understanding the hydrological cycle and ~~water resources~~ present state of water resources. These
59 key scientific issues can be ~~addressed~~ resolved by investigating the ~~spatiotemporal~~ spatial and

60 ~~temporal~~ distribution and ~~control~~~~driving~~ mechanisms of surface ~~water~~ and groundwater resources
61 ~~in~~ ~~within~~ the basin under accelerating ~~climate change~~~~climate warming~~.

62 The Tibetan Plateau, ~~also~~ known as the “Third Pole”, has complex ~~cryospheric~~~~cryosphere-~~
63 ~~hydrologic~~~~hydrology-~~geodynamic processes and is especially ~~susceptible~~~~vulnerable~~ to global
64 warming (Zhang et al., 2017; Yao et al., 2022). ~~The Qaidam Basin in the northeastern Tibetan~~
65 ~~Plateau is the area that has warmed the most in the entire Tibetan Plateau~~~~The Qaidam Basin is~~
66 ~~situated in the northeastern Tibetan Plateau and presents the largest extent of warming in the entire~~
67 ~~Tibetan Plateau and a substantial steep rise in temperature globally~~ (Li et al., 2015; Kuang and
68 Jiao, 2016; Yao et al., 2022). Since 1961, the average temperature of the basin has ~~increased~~~~been~~
69 ~~rising~~ at an alarming rate of 0.53°C ~~per decade~~~~10 a~~ ~~caused by~~~~as a result of~~ climate warming (Wang
70 et al., 2014), resulting in ~~an~~ ~~increased~~ ~~in~~ precipitation and ~~cryospheric~~ retreat ~~of the cryosphere in~~
71 ~~the region~~ (Song et al., 2014; Xiang et al., 2016; Zou et al., 2022; Wang et al., 2023). These changes
72 have led to ~~drastic~~~~rapid~~ spatial changes in ~~surface water and ground~~water storage ~~in the Qaidam~~
73 ~~Basin, increased~~~~increasing~~ runoff ~~or rising groundwater table over wide areas in most parts of the~~
74 ~~region~~ (Jiao et al., 2015; Wei et al., 2021), and hydrological changes, ~~such as the expansion of~~
75 ~~lakes,~~ in the central and northern ~~regions of the basin, such as the lakes expansion~~ (Ke et al., 2022;
76 Zhang et al., 2022). However, several questions remain to be ~~resolved~~~~answered~~: How are
77 hydrological changes in the basin driven by climate changes? What are the potential influences of
78 these changes on the water resources of the basin? ~~The dynamics of surface water and groundwater,~~
79 ~~which link precipitation and meltwater from high elevations with the low-lying lake basins,~~
80 ~~provide evidence of the effects of climate change on water cycle processes. These issues require~~
81 ~~an in-depth investigation. Rivers and groundwater carry precipitation and meltwater from high-~~
82 ~~altitude areas to the lakes in low-lying areas; information on climate hydrology dynamics of the~~
83 ~~runoff process can provide key evidence for the entire water cycle process. Hence, t~~~~The Qaidam~~
84 Basin is ~~therefore~~ an excellent site ~~for~~ ~~to~~ reveal the mechanisms of global warming-induced
85 responses to the hydrological cycle on the Tibetan Plateau ~~investigating the response mechanism~~
86 ~~of the hydrological cycle in the Tibetan Plateau caused by global warming~~.

87 ~~The isotopes of hydrogen and oxygen are useful~~ Water isotopes (H and O) represent important
88 ~~components of water molecules and are useful natural environmental tracers of~~ ~~for~~ the water cycle
89 and climate reconstruction, ~~and, they~~ ~~They~~ can help elucidate the processes that control water
90 cycle changes, thus providing scientific evidence for human adaptations and effects on future

91 global changes (Craig, 1961; Dansgaard, 1964; Yao et al., 2013; Bowen et al., 2019; Kong et al.,
92 ~~2019; Zhu et al., 2023~~). ~~Stable w~~Water isotope records provide key information on water
93 ~~flowmigration processes~~, and they can compensate for the paucity of hydrometeorological,
94 geological, and borehole data in hydrological research. Stable H-O isotopes and radioactive ^3H
95 isotopes have been widely applied to quantify surface ~~water~~ or groundwater recharge sources,
96 interactions, budgets, and ages (Befus et al., 2017; Stewart et al., 2017; Moran et al., 2019; Bam
97 et al., 2020; Rodriguez et al., 2021; Shi et al., 2021; Ahmed et al., 2022; Benettin et al., 2022).
98 Previous researchers have also performed a substantial amount of work on ~~the use of using~~ isotopes
99 to ~~delineatetraee~~ the water cycle in the Qaidam Basin (Xu et al., 2017; Xiao et al., 2017, 2018;
100 Zhao et al., 2018; Tan et al., 2021; Yang and Wang, 2020; Yang et al., 2021). These studies have
101 enhanced our understanding of aquifer properties in local regions and ~~their~~ recharge mechanisms.
102 However, ~~past assessments of the water cycle in the Qaidam Basin have been constrained by the~~
103 ~~challenges of the harsh natural conditions and scarce of hydrogeological data under the constraints~~
104 ~~of the harsh climate environment and hydrogeological survey accessibility in the Qaidam Basin,~~
105 ~~the water cycle processes in the basin in previous reports are mainly understood based on the~~
106 ~~watershed or confined regional unit scale. It is a great challenge~~The use of regional research to
107 achieve a comprehensive elucidation of the basin-scale water cycle mechanism ~~is a challenge~~.
108 Furthermore, ~~the surface water and groundwater~~ seasonal recharge ~~information~~ of the whole basin
109 has not been systematically explored. ~~Various hydrological, climatic, and hydrogeological~~
110 ~~conditions of the basin are caused by~~ ~~Continuous-continuous~~ changes in the topographical and
111 tectonic spatial patterns ~~of the basin are caused by various hydrological, climatic, and~~
112 ~~hydrogeological conditions~~; moreover, the hydrological effects exerted by anthropogenic climate
113 change ~~and regional aquifer properties~~ differ seasonally (Jasechko et al., 2014). Therefore, it is
114 ~~urgent particularly essential~~ to ~~develop a comprehensive understanding study the entire process~~ of
115 ~~the~~ basin water cycle and ~~its~~ seasonal changes. While carrying out a comprehensive assessment of
116 differences in ~~isotopic composition isotopes~~ of various potential recharge sources, it is fundamental
117 to use the same technical methods for the systematic sampling and isotopic characterization of the
118 basin.

119 In this study, ~~we constrain the hydrological cycle of the Qaidam Basin and surrounding~~
120 ~~mountains using stable H-O and radioactive ^3H isotope data collected during the wet and dry~~
121 ~~seasons from eight study sites in the eight major watersheds in the basin of the Qaidam Basin were~~

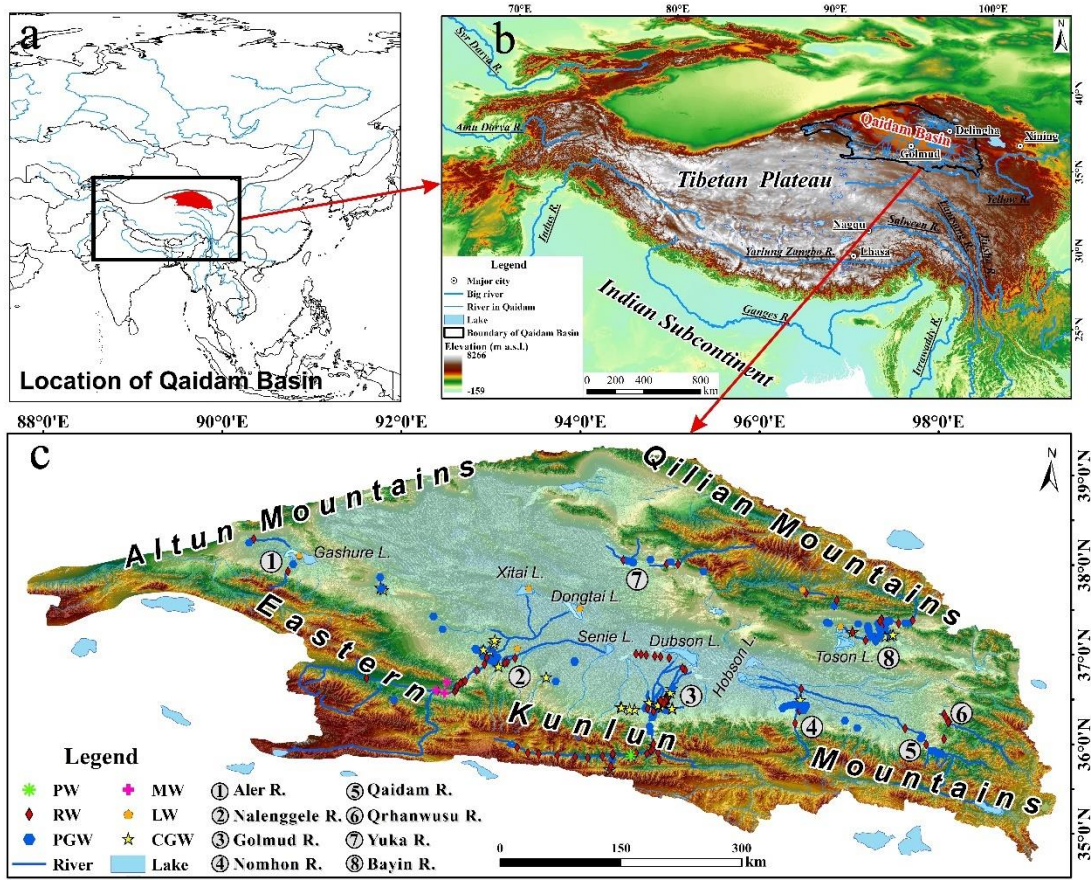
selected as the study sites, and constraints were placed on the hydrological cycle patterns and processes of the Qaidam Basin based on stable H-O isotope and radioactive ^3H isotope data from the wet-dry season. The study aims are: 1) to elucidate the spatial-seasonal distribution pattern of surface water and groundwater isotopes at different watershed scales in this alpine arid basin at various spatial and seasonal scales; 2) analyze the composition changes of the Qaidam Basin water sources at different spatial-seasonal scales; 3) to identify and quantify the main components of the regional water cycle, their timing and spatial heterogeneity; trace the entire water cycle process around the mountain-basin watersheds of the Qaidam Basin; and 4) to reveal isotopic hydrological responses to climate change and to predict the trend in the changes of Qaidam Basin water resources under the influence of a large extent of climate warming. The scientific contributions of this study include clarifying the isotope hydrology responses to climate change in the Tibetan Plateau arid basin, which is one of the ecosystems most affected by climate warming worldwide, from a microscopic scale; predicting the changing trend of water resources under the condition of multiple water sources recharge; and elucidating the entire water cycle process in extremely arid basins under the influence of rapid climate change.

2. Study area

2.1. General features

The Qaidam Basin is a closed and huge fault-depression basin situated in the northeastern Tibetan Plateau surrounded by the Kunlun, Qilian and Altun Mountains (Figures 1a and 1b). The basin is one of the four main basins in China. With an area of approximately 250,000 km², the basin is one of the four main basins in China, and it is surrounded by the Kunlun Mountains, Qilian Mountains and Altun Mountains. The Qaidam Basin has a plateau continental climate and represents a typical alpine arid inland basin that is characterized by drought. There are significant temperature variations in the basin, and the average annual temperature is below 5 °C. The annual precipitation declines from 200 mm in the southeastern region to 15 mm in the northwestern region. The average annual relative humidity is 30%–40%, with a minimum of less than 5%. Modern glaciers have formed in the mountains on the western, southern and northeastern sides of the basin. The basin is surrounded by more than 100 rivers. Approximately about

152 10 rivers of which are perennial/permanent, with most of the local rivers representing being
 153 intermittent river systems. The rivers are mainly distributed on the eastern side of the basin but
 154 seant-are scarce on the western side. The water in the basin's lakes has-becomeis predominantly
 155 saline, with a total of comprising 31 salt lakes in total.



156
 157 **Figure 1.** Location of Qaidam Basin (a, b) and the sampling sites (c).

158 **2.2 Basic hydrogeological setting** Hydrogeology and structure

159 The basin basement consists of Precambrian crystalline metamorphic rock series, and the
 160 caprock is of Paleogene-Neogene and Quaternary strata. The mountainous area surrounding the
 161 basin is dominated by a Paleogene system, and the basin area and basin boundary zone are
 162 characterized by a wide distribution of the Paleogene-Neogene system. The Quaternary system is
 163 mainly distributed in the central basin region and the intermountain valley region. The basin terrain
 164 is slightly tilted from the northwest to southeast, and the height gradually reduces from 3000 m to
 165 approximately 2600 m. The distribution of the basin landforms presents-shows a concentric ring

166 shape. From the ~~edge-rim~~ to the ~~center-centre~~, the distribution of diluvial gravel fan-~~shaped-land~~
167 (Gobi), alluvial-diluvial silt plain, lacustrine-alluvial silt clay plain, and lacustrine silt-salt plains
168 follow a regular pattern. Salt lakes are extensively distributed in ~~the lowlands-low-lying-terrains~~.
169 The inner edge of the Gobi belt in the northwestern basin region is clustered with hills that are less
170 than 100 m in height. The southeastern region of the basin has ~~pronounced-marked~~ subsidence, and
171 the alluvial and lacustrine plains are ~~extensive-expansive~~. In the northeastern basin-~~region~~, a
172 secondary small intermountain basin has been formed between the basin and the Qilian Mountains
173 by the uplifting of a series of low mountain fault blocks of metamorphic rock series.

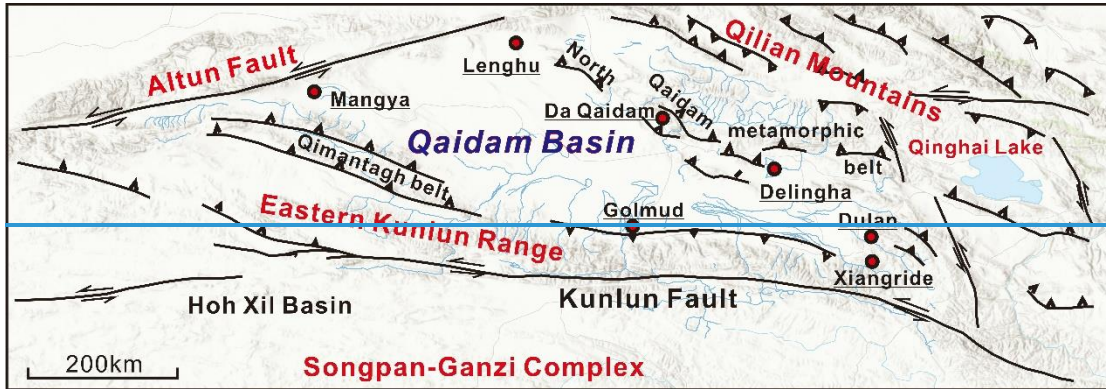
174 The Qaidam Basin is ~~located-situated~~ in the Qin-Qi-Kun tectonic system, where there is strong
175 neotectonic movement, and a series of syncline-anticline tectonic belts and regional deep faults
176 have formed around it. The fault structures in the Qaidam Basin are very well developed and
177 include the north-easterly ~~Altun-Alun~~ fault in the north; north-westerly Saishenteng-Aimunik
178 northern margin deep fault in the northeast; westerly Qaidam northern margin deep fault in the
179 northwest; Qimantag Mountains and Burhan Budai Mountains-Aimunik northern margin deep
180 fault in the south; and north-westerly Sanhu major fault and north-easterly Qigaisu-Dongku Fault
181 in the central basin region.

182 The ~~distribution of surface water in the basin~~ ~~basin-water-system distribution~~ is ~~constrained~~
183 ~~by-subject-to-the-constraints-of-the~~ topography and neotectonic movements, and ~~it~~ appears to
184 ~~present-have-a-general-an-overall~~ centripetal radial pattern (Figure 1c). There is ~~widespread-frequent~~
185 surface water- ~~and~~ groundwater exchange-. ~~The mountainous areas are rich in precipitation and~~
186 ~~ice/snow meltwater, and are the main runoff producing areas, which is generally manifested as an~~
187 ~~abundance of precipitation and ice/snow meltwater in the mountainous areas, which are the main~~
188 ~~runoff areas. The r~~Runoff from the mountains flows through the Gobi belt ~~in front of the mountain,~~
189 ~~with-where~~ most of it ~~infiltrating-infiltrates~~ into the groundwater ~~system,-~~ ~~subsequently~~
190 ~~Groundwater discharges to~~flows over the surface ~~from springs in in the form of~~ confined ~~artesian~~
191 ~~water-aquifers~~ or a ~~spring~~s at the front edge of the alluvial fan-, ~~and-This water~~ finally flows into
192 ~~the~~ terminal lakes.

193 Groundwater can be roughly ~~divided-classified~~ as: i) ~~into-fractured-bedrock water-bedrock~~
194 ~~fissure-water;~~ ii) leached pore water and local confined groundwater; ~~iii)~~ phreatic groundwater
195 and confined artesian water-, ~~as-well-as;~~ iv) ~~saline-salty~~ phreatic groundwater; ~~v)~~ brine, and

196 salinity confined artesian water. Surface water and groundwater salinity and solutes are
 197 gradually enriched along the flow path this process (Figure 2; Wang et al., 2008).

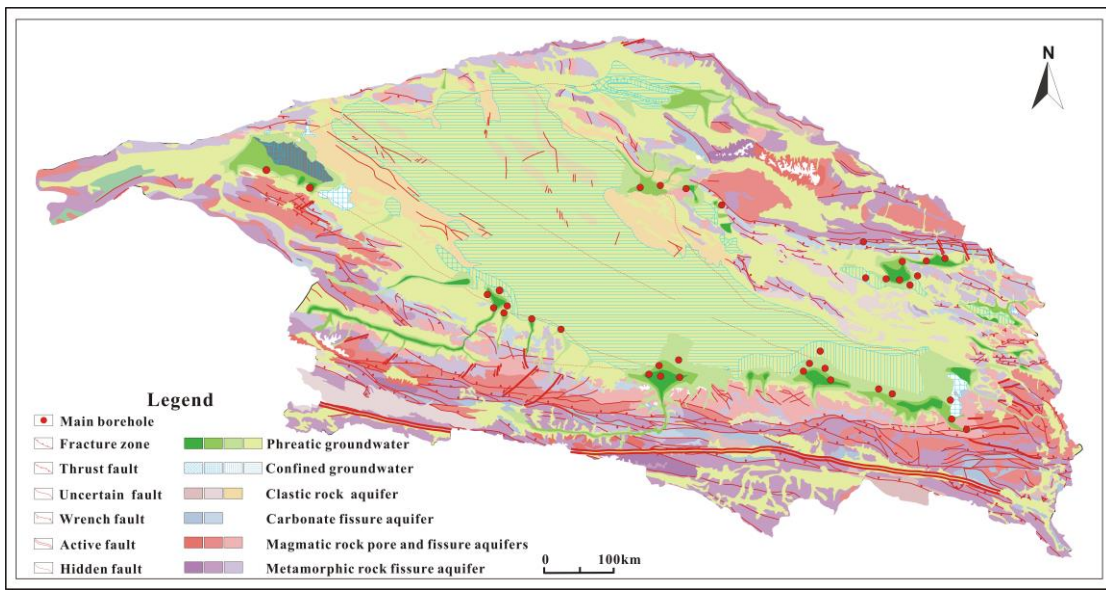
198



199



200



201 **Figure 2.** Hydrogeologic map of the Qaidam Basin (Modified from Xi'an Center, China Geological Survey,
 202 <http://www.xian.cgs.gov.cn/>). The color of different patches of the same aquifer, from dark to light, denotes high
 203 to low in water yield property, tectonic distribution (modified after Jian et al., 2020)

204 3. Sampling and methods

205 3.1 Sampling and analysis

206 ~~We collected To elucidate the water cycle mechanisms in the Qaidam Basin, field~~
207 ~~investigations and samplings were carried out on the~~from 8 major river-groundwater systems in
208 the region from 2019 to 2021. ~~We collected samples from The sampling frequency of 6 watersheds~~
209 ~~of the systems onceessentially extends over~~a hydrological year, ~~and is consisting of~~represented
210 ~~by~~ the wet season (July–August) and the dry season (March–April). Precipitation and snow
211 meltwater were collected from the Eastern Kunlun Mountains. ~~Snow meltwater was collected in~~
212 ~~the dry season whereas precipitation was collected at several times during a hydrological year.~~ In
213 total, 239 sampling points were established: ~~phreaticphreic~~ groundwater (n = 100), confined
214 groundwater (n = 43), spring water (n = 6), river water (n = 81), lake water (n = 5), snow meltwater
215 (n = 3), and precipitation (n= 1). A total of 422 sets of samples were collected. No sampling point
216 was established in the northwestern basin because the southern slope and front edge of the Altun
217 Mountains consisted of ~~tertiary-Tertiary~~ system halite sedimentation and Quaternary system ~~large~~
218 ~~thick~~ salt flats, and no freshwater body ~~is was developed~~present. Therefore, the sample collection
219 covers the entire Qaidam Basin and each of the major endorheic regions.

220 Hydrogen and oxygen isotopes (^2H , ^3H , and ^{18}O) ~~tests~~ were ~~conducted-analyzed~~ at the State
221 Key Laboratory of Hydrology-Water Resources and Hydraulic Engineering, Hohai University,
222 China. A MAT253 mass spectrometer was used to measure the ratios of $^2\text{H}/^1\text{H}$ and $^{18}\text{O}/^{16}\text{O}$, and
223 the results were compared with the Vienna Standard Mean Ocean Water (VSMOW), expressed in
224 δ (‰), with the analytical precision (1σ) of the instrument for these isotopes was lower than $\pm 1\%$
225 and $\pm 0.1\%$. To determine the tritium (^3H) concentration, the water sample was first concentrated
226 by electrolysis. Following sample enrichment, measurements were carried out using low
227 background liquid scintillation counting (TRI-CARB 3170 TR/SL). The findings were expressed
228 in terms of absolute concentration in tritium units (TU), the detection limit of the instrument was
229 0.2 TU, and the precision was improved to ~~more-less~~ than ± 0.8 TU.

230 3.2 Hydrograph separation

231 In the analysis of water sources among hydrological processes, endmember mixing models
232 are widely used. ~~The contribution of each recharge endmember to the mixed water body was~~

233 ~~estimated with a Bayesian mixing model that considers~~According to the heterogeneity of different
234 end-member isotopes/water chemistry parameters,~~combined with the Bayesian mixing model, the~~
235 ~~contribution of each recharge end member to the mixed water body can be estimated~~ (Hooper et
236 al., 1990, 2003; Chang et al., 2018). The process is as follows:

$$1 = \sum_{i=1}^n f_i, \quad C_m^j = \sum_{i=1}^n f_i C_i^j, \quad j = 1, \dots, n \quad (1)$$

238 where f_i represents the proportion of water source i , n represents the number of end-members, and
239 C_m^j represents the level of tracer j in end-member i .

240 ~~The Stable isotope analysis in R based on~~Bayesian mixing models (MixSIAR) ~~coded in R~~
241 can quantify the contributions of more than two potential endmembers (Parnell et al., 2010). In
242 this study, based on the differences in the water body properties and isotopic composition of each
243 endmember, $\delta^{18}\text{O}$, δD , and d-excess (d-excess = $\delta\text{D} - 8\delta^{18}\text{O}$) data were used as parameters in the
244 modeling. The model ~~was calculated~~~~calculation process was carried out~~ at a fractional increment
245 of 1% and an uncertainty level of 0.1%.

246 3.3 Water vapor trajectory

247 The source and transport route of moisture can be monitored based on the water vapor flux
248 field derived from the monthly mean ERA5 reanalysis data ($0.25^\circ \times 0.25^\circ$) of the European Centre
249 for Medium-Range Weather Forecasts (ECMWF, <https://www.ecmwf.int/>) (Hersbach et al., 2019).
250 ~~In this study, a~~After taking into account that more than 70% of the precipitation in the Qaidam
251 Basin occurs from June to September, the monthly mean ERA5 reanalysis data in this period from
252 2019 to 2021 were used to analyze the water vapor transport path in and around the study area.
253 Based on the average altitude of >3000 m at the study site, the simulated atmospheric pressure was
254 set to 500 hPa. The majority of the atmospheric water vapor was distributed in the range of 0–2
255 km above ground, and the simulated height did not have any ~~significant~~~~remarkable~~ influence on
256 the findings (Li and Garziona, 2017; Yang and Wang, 2020).

257 4. Results

258 4.1 Stable H and O isotopes of different water bodies

259 The spatiotemporal changes of isotopes in the various water bodies in the entire basin are
260 large, the watersheds have distinct characteristics, and considerable differences exist between
261 surface water and groundwater. The $\delta^{18}\text{O}$ and δD values extracted from the water samples of each
262 watershed in the study region can be classified into six categories (Figure 3): 1) precipitation; 2)
263 snow meltwater; 3) river water; 4) lake water; 5) phreatic groundwater; and 6) confined
264 groundwater.

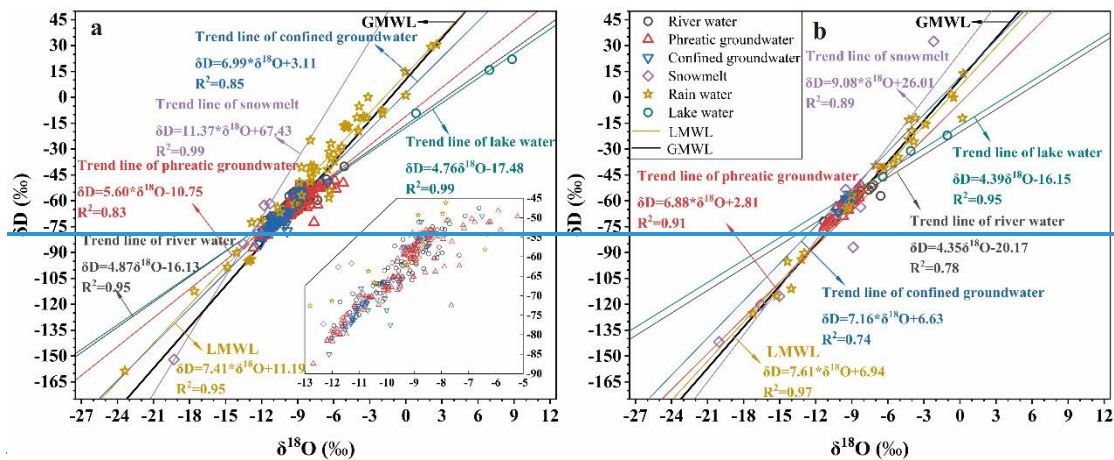
265 In the Qaidam Basin, the sources of precipitation are mainly concentrated on the northern and
266 southern slopes of the Kunlun Mountains and Qilian Mountains, respectively. The ranges of $\delta^{18}\text{O}$
267 and δD of the precipitation samples from the Kunlun Mountains and Qilian Mountains (Zhu et al.,
268 2015) were -23.38‰ to $+2.55\text{‰}$ and -158.64‰ to $+30.49\text{‰}$, respectively. The corresponding
269 fitted Local meteoric water line (LMWL) equation in the Qaidam Basin was $\delta\text{D} = 7.48\delta^{18}\text{O} +$
270 11.30 ($R^2 = 0.95$, $n = 74$), where the slope and intercept were similar to the long-term monitoring
271 findings of the Qilian Mountains (Zhao et al., 2011; Gui et al., 2020; Wu et al., 2022; Yang et al.,
272 2023). In the Qaidam Basin, the heavy isotopes present in snow meltwater samples were
273 considerably depleted compared to rainwater. The $\delta^{18}\text{O}$ and δD ranges were -19.30‰ to -8.27‰
274 and -152.02‰ to -53.52‰ respectively, and the fitting trend equation was $\delta\text{D} = 7.78\delta^{18}\text{O} + 10.85$
275 ($R^2 = 0.83$, $n = 11$), with the slope and intercept lying between LMWL and GMWL (Global
276 meteoric water line).

277 Among the surface water samples, the $\delta^{18}\text{O}$ and δD ranges in river water were -13.51‰ to
278 -5.93‰ and -85.00‰ to -47.50‰ respectively, whereas those in the lake water were more
279 enriched at -4.10‰ to 8.84‰ and -31.05‰ to 22.07‰ , respectively. The fitted trend lines of river
280 and lake samples were: $\delta\text{D} = 5.97\delta^{18}\text{O} - 5.54$ ($R^2 = 0.85$, $n = 92$) and $\delta\text{D} = 4.64\delta^{18}\text{O} - 16.37$ (R^2
281 $= 0.99$, $n = 7$), respectively, which were below both the GMWL and LMWL, indicating that the
282 surface water body has undergone varying extents of evaporation, with evaporation from lakes
283 being more enhanced.

284 In the groundwater samples, the H-O isotopic composition range was wider and considerable
285 differences occurred between phreatic and confined groundwater. The $\delta^{18}\text{O}$ and δD value

286 distribution ranges in phreatic groundwater were -12.70‰ to -5.21‰ and -87.38‰ to -42.00‰ ,
 287 respectively, and the fitted trend line was $\delta D = 5.73\delta^{18}O - 9.20$ ($R^2 = 0.83$, $n = 185$). The phreatic
 288 groundwater isotopic composition and slope of the trend line were similar to those of surface water,
 289 indicating frequent interactions between the two and substantial evaporative fractionation of some
 290 shallow groundwater. The $\delta^{18}O$ and δD ranges in confined groundwater were relatively small and
 291 lower in comparison at -12.12‰ to -8.58‰ and -85.00‰ to -51.01‰ . The linear regression
 292 relationship of the samples fitting ($\delta D = 7.84\delta^{18}O + 12.39$, $R^2 = 0.87$, $n = 51$) revealed that its
 293 slope and intercept were essentially consistent with those of GMWL and LMWL, which suggests
 294 the presence of a strong correlation between confined groundwater and atmospheric precipitation
 295 in different periods.

296 Overall, in the Qaidam Basin, the stable H-O isotopic compositions of surface water and
 297 groundwater were generally positively skewed. The isotopic composition and trend fitting
 298 characteristics both demonstrated that the water samples have undergone varying extents of
 299 evaporation during runoff, which reflects the cold and dry climate environmental characteristics
 300 of the study area.

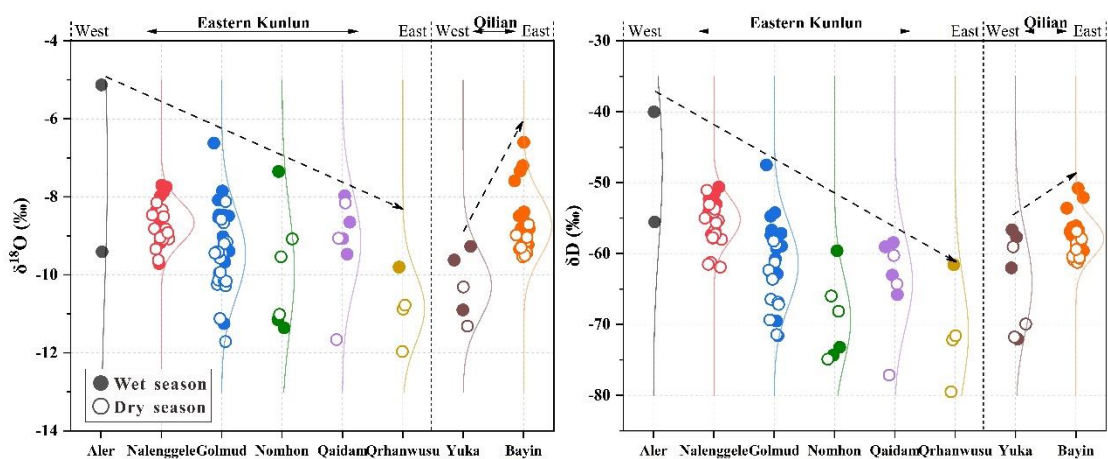


301
 302 **Figure 3.** Diagram showing the relationship between $\delta^{18}O$ and δD in different water bodies in the Qaidam Basin
 303 (a. Eastern Kunlun Mountains water system; b. Qilian Mountains water system; The data of Rain water and
 304 Snowmelt in the Qilian Mountains were from Zhu et al., 2015 and Yang et al., 2021, respectively)

305 4.2-1 Spatial and seasonal characteristics of surface water $\delta^{18}O$ - δD

306 In the Qaidam Basin, considerable spatial seasonal and seasonal spatial variations exist
 307 in the stable H-O isotopes of surface water (Figure 43). The isotopic compositions of rivers

308 originating from the Eastern Kunlun Mountains contrast with those from and Qilian Mountains
 309 had shown, where the heavy isotopes of the Eastern Kunlun Mountains are gradually depleted in
 310 the direction of west to east, and the reverse holds true for the Qilian Mountains. Of these, the $\delta^{18}\text{O}$
 311 and δD values are significantly positive in the southwestern basin and, while significantly negative
 312 in the eastern basin. In terms of seasonal variation, a Apart from the Nomhon River, all watersheds
 313 exhibit displayed the a characteristics seasonal variation of enriched in heavy isotope enrichment
 314 to varying extents during the wet season relative to the and relative depletion during the dry season.
 315 The basin surface water mean $\delta^{18}\text{O}$ and δD values in surface water were are more
 316 positively positively skewed by -0.08‰ to 1.08‰ and 0.63‰ to 10.586‰ , respectively, in the wet
 317 seasons. Moreover, the seasonal variations of $\delta^{18}\text{O}$ and δD were are more evident pronounced in
 318 the downstream river compared to the upstream segment. For instance, example, the $\delta^{18}\text{O}$ value of
 319 the downstream Nomhon River was is 3.66‰ higher during the wet season compared to the dry
 320 season. These phenomena reflect the differences in the recharge sources of the river during both
 321 the wet and dry seasons and the strong surface evaporation effect in the central basin region. For
 322 spatial patterns, the isotopic composition of rivers originating from the Eastern Kunlun Mountains
 323 and Qilian Mountains had a contrasting distribution pattern, where the heavy isotopes of the
 324 Eastern Kunlun Mountains are gradually depleted in the direction of west to east, and the reverse
 325 held true for the Qilian Mountains. Of these, the $\delta^{18}\text{O}$ and δD values were significantly positively
 326 skewed in the southwestern region of the basin and significantly negatively skewed in the eastern
 327 region.

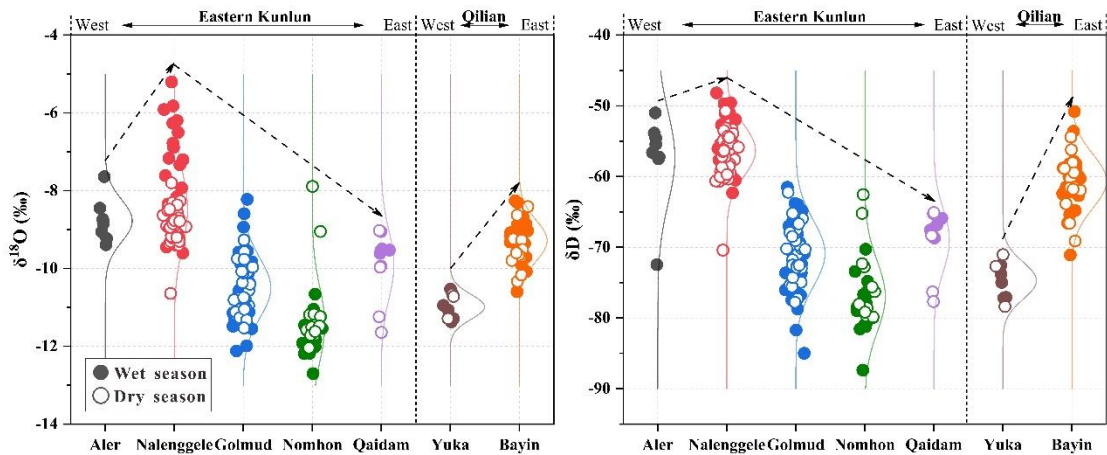


328

329 **Figure 43.** ~~Spatiotemporal~~ Spatial and temporal variations in the H-O isotope composition of Qaidam Basin river
330 water. ~~(Filled and hollow dots indicate wet and dry seasons, respectively; \pm The light lines indicate the trend of~~
331 ~~$\delta^{18}\text{O}$ and δD values from west to east).~~

332 4.3-2 ~~Spatial-~~ and seasonal characteristics of groundwater $\delta^{18}\text{O}$ - δD

333 The spatial variability of groundwater stable H-O isotopes ~~was~~ is more pronounced compared
334 with river water, although it ~~did~~ appears to follow the same distribution pattern as river water in
335 the ~~watershed-basin~~ (Figure 54). ~~In terms of seasons,~~ The $\delta^{18}\text{O}$ and δD values in ~~the~~ groundwater
336 system ~~were~~ are lower and seasonal fluctuations were smaller compared to ~~that~~ those of in the
337 surface water. ~~because the kinetic fractionation of isotopes caused by evaporation and mixing are~~
338 weaker in groundwater than in surface water. Specifically, the average seasonal variation of $\delta^{18}\text{O}$
339 in each of the groundwater systems ~~was in the range~~ of from -0.75‰ to $+0.84\text{‰}$, and the
340 ~~largest~~ maximum seasonal variations in individual ~~borehole-boreholes~~ were are $+3.31\text{‰}$ and
341 -3.16‰ , respectively. This ~~suggests~~ indicates that the groundwater reflects a spatial and temporal
342 average of the surface water isotopic signal, and averaging reduces the variability of the
343 values ~~groundwater isotopic composition was not entirely impacted by surface water infiltration.~~
344 The region with the ~~greatest~~ largest seasonal fluctuations of groundwater ~~was~~ is located in the
345 Nalenggele River ~~in the~~ , southwestern basin, and the groundwater ~~$\delta^{18}\text{O}$ and δD~~ stable H-O isotopes
346 in wet season ~~were~~ are noticeably significantly more positively skewed compared to those ~~of in the~~
347 dry season. This indicates that groundwater is flowing rapidly and each season, new infiltration
348 displaces the earlier infiltration. ~~Meanwhile,~~ the adjacent Golmud River, however, has the ~~the~~
349 ~~region with the smallest~~ least seasonal variations ~~of in~~ $\delta^{18}\text{O}$ and δD ~~is the adjacent Golmud River.~~
350 In contrast, this suggests that flow is slow. Although there ~~were~~ are no ~~obvious~~ apparent differences
351 in the topography and landforms ~~of between~~ the two adjacent watersheds, significant differences
352 ~~were~~ are observed in the isotope signatures ~~isotopic characteristics~~ of the two, where both surface
353 water and groundwater show much more positive $\delta^{18}\text{O}$ and δD values in the Nalenggele River than
354 that of Golmud River catchment. ~~These phenomena reflect the following: 1) the kinetic~~
355 ~~fractionation of groundwater isotopes caused by evaporation and mixing was smaller than that of~~
356 ~~surface water isotopes; and 2) substantial differences were detected between the groundwater~~
357 ~~recharge and surface water groundwater hydraulic interactions in each watershed.~~



358

359 **Figure 54.** Spatiotemporal Spatial and temporal variations in H-O isotopes in the groundwater of the Qaidam
 360 Basin. Filled and hollow dots indicate wet and dry seasons, respectively; The light lines indicate the trend of
 361 $\delta^{18}\text{O}$ and δD values from west to east.

362 4.3 Isotopic variations in different water bodies

363 In the Qaidam Basin, the ranges of $\delta^{18}\text{O}$ and δD of the precipitation samples from the Kunlun
 364 Mountains and Qilian Mountains are -23.38‰ to $+2.55\text{‰}$ and -158.6‰ to $+30.5\text{‰}$, respectively
 365 (Table S1; Zhu et al., 2015). The fitted local meteoric water line (LMWL) equation in the Qaidam
 366 Basin is $\delta\text{D} = 7.48\delta^{18}\text{O} + 11.30$ ($R^2 = 0.95$, $n = 74$), where the slope and intercept are similar to
 367 the long-term monitoring findings of the Qilian Mountains (Figure 5; Zhao et al., 2011; Juan et al.,
 368 2020; Wu et al., 2022; Yang et al., 2023). In the Qaidam Basin, the heavy isotopes present in snow
 369 meltwater samples are considerably depleted compared to rainwater (Clark and Fritz, 2013). The
 370 $\delta^{18}\text{O}$ and δD ranges are -19.30‰ to -2.19‰ and -152.0‰ to 32.4‰ respectively, and the fitting
 371 trend equation was $\delta\text{D} = 9.21\delta^{18}\text{O} + 31.78$ ($R^2 = 0.89$, $n = 12$), with the slope and intercept greater
 372 than LMWL and GMWL (Global meteoric water line).

373 The $\delta^{18}\text{O}$ and δD ranges in river water are -13.51‰ to -5.93‰ and -85.0‰ to -47.5‰
 374 respectively, whereas those in the lake water are more enriched at -4.10‰ to 8.84‰ and -31.1‰
 375 to 22.1‰ , respectively (Figure 5). The fitted trend lines for river and lake samples are: $\delta\text{D} =$
 376 $5.97\delta^{18}\text{O} - 5.54$ ($R^2 = 0.85$, $n = 92$) and $\delta\text{D} = 4.64\delta^{18}\text{O} - 16.37$ ($R^2 = 0.99$, $n = 7$), respectively,
 377 which are below both the GMWL and LMWL, indicating varying extents of evaporative
 378 fractionation in the surface water bodies, with evaporation from lakes being more enhanced. The
 379 radioactive ^3H concentrations range from 4.2 to 17.8 TU, with a mean value of 12.93 TU ($n=23$,
 380 Table S1).

381 The H-O isotopic composition ranges in the groundwater samples are wider and considerable
382 differences are observed between phreatic and confined groundwater (Figure 5). The $\delta^{18}\text{O}$ and δD
383 values range in phreatic groundwater from -12.70‰ to -5.21‰ and -87.4‰ to -42.0‰ ,
384 respectively. The fitted trend line is $\delta\text{D} = 5.73\delta^{18}\text{O} - 9.20$ ($R^2 = 0.83$, $n = 185$). The phreatic
385 groundwater isotopic composition and slope of the trend line are similar to those of surface water,
386 indicating considerable interactions between the two and substantial evaporative fractionation of
387 some shallow groundwater. The $\delta^{18}\text{O}$ and δD ranges in confined groundwater are relatively small
388 and lower in comparison at -12.12‰ to -8.58‰ and -85.0‰ to -51.0‰ . The linear regression
389 relationship of the samples fitting ($\delta\text{D} = 7.84\delta^{18}\text{O} + 12.39$, $R^2 = 0.87$, $n = 51$) revealed that its
390 slope and intercept were essentially consistent with those of GMWL and LMWL, suggesting the
391 presence of a strong correlation between confined groundwater and atmospheric precipitation in
392 different periods. Radioactive ^3H concentrations detectable in the phreatic and confined
393 groundwater range from 0.22 to 30.35 TU and 0.60 to 12.76 TU, respectively, with mean values
394 of 10.23 TU ($n=49$) and 7.55 TU ($n=10$), respectively (Table S1).

395 Overall, the stable H-O isotopic compositions of surface water and groundwater are generally
396 more enriched in the Qaidam Basin. The isotopic compositions and trend fitting features both
397 demonstrated that the water samples have undergone varying degrees of evaporation during runoff,
398 indicating the cold and dry climate environmental characteristics of the study area.

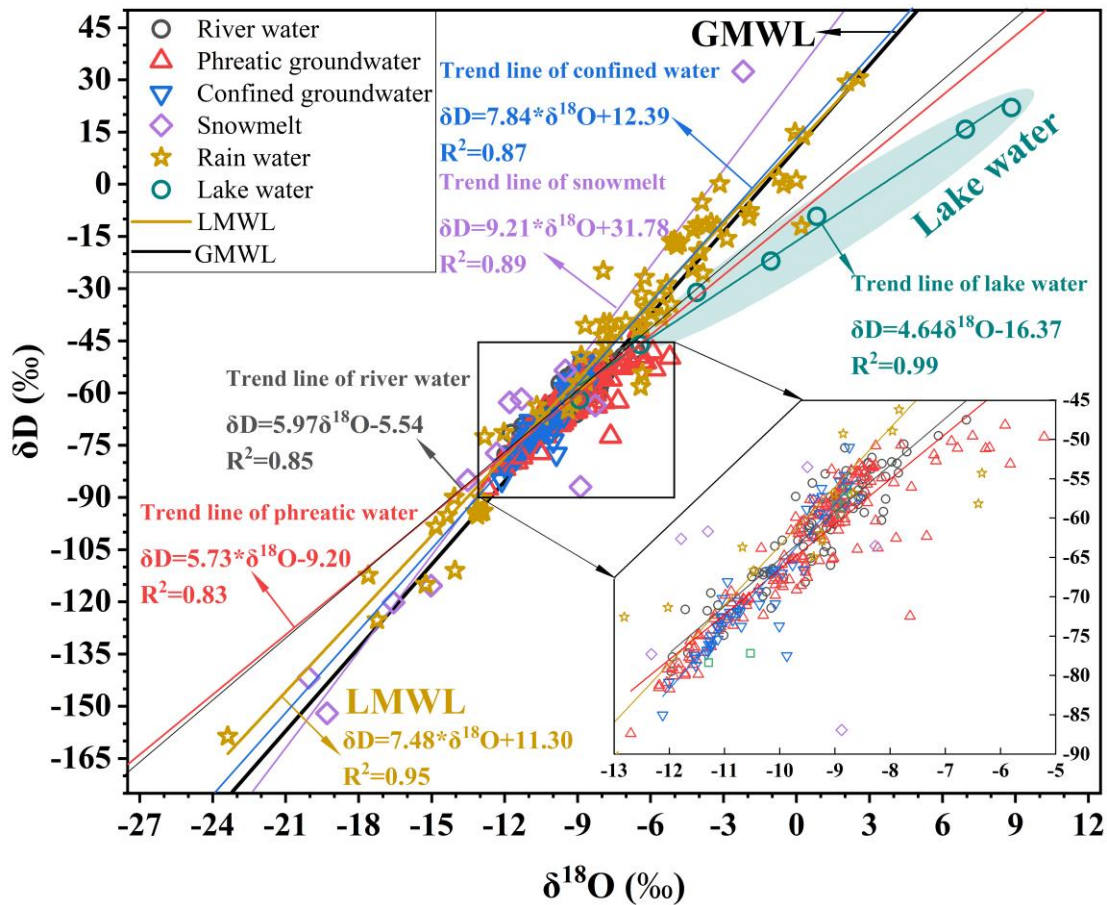


Figure 5. Plot of the relationships between $\delta^{18}\text{O}$ and δD in different water bodies from the Qaidam Basin.

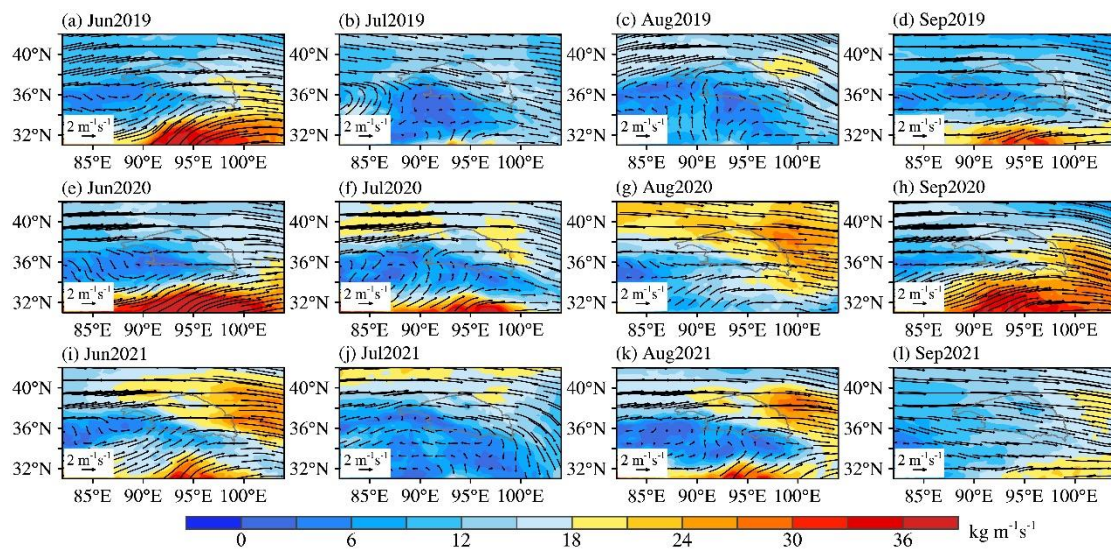
5. Discussion

5.1 Water cycle information indicated by surface water isotopes

5.1.1 Atmospheric moisture transport pattern

To further explain the cause of seasonal-spatial and seasonal spatial-variations of surface water $\delta^{18}\text{O}$ and δD values, ERA5 reanalysis data in the rainy season (June to September) were used to calculate the water vapor flux field in the Qaidam Basin and its surrounding areas as well as track the main trajectoriespaths of the moisturewater vapor transportation of precipitation (Hersbach et al., 2019). The results show that the mid-latitude westerlies dominate the moisturewater vapor paths inside and around the basin, and the water vapor flux in the eastern region of the basin is notably greater than that in the western basin (Figure 6; Yang and Wang, 2020)region. This largely explains the spatial change-patterns of river water H-O isotopes (Figure

3), as well as hydrothermal condition temperature and precipitation regimes to a large degree (Figure S1). Atmospheric and isotopic tracing data also support these conclusions. For instance, example, the Tanggula Mountains (33°–35° N) serve as the physical and chemical boundary of the Tibetan Plateau, and the westerlies fundamentally govern the northern region, preventing the Indian monsoon from having a significant impact on the Qaidam Basin (Yao et al., 2013; Kang et al. 2019; Wang et al., 2019). Furthermore, d-excess can effectively represent the moisture source properties where the recycled moisture that enhanced by evaporation over the land surface evaporated under conditions of low humidity and moisture water characterized carried by the westerlies westerly wind is are considered to possess higher d-excess values. The mean d-excess of basin river water samples during the wet season (11.45‰, Table S1) was greater than 10‰, which reflects associated with the characteristics of an alpine arid continental climate and a moisture water vapor source devoid of monsoon influences. Higher d-excess values are attributed to westerlies moisture and recycled moisture that is boosted by inland surface evaporation. In contrast, the hinterland of the Tibetan Plateau, south of the Tanggula Mountains, which was subject to significant influences from the Indian monsoon circulation, had summer precipitation and river water d-excess values that ranged from 5‰ to 9‰ with a mean value of 7‰ (Tian et al., 2001). The stark contrasts in the d-excess values between the two regions further support the above inference about the moisture water vapor sources of the Qaidam Basin.



430
 431 **Figure 6.** Tropospheric water vapor flux from June to September 2019 to 2021 (below 500 hPa, unit: $\text{kg m}^{-1}\text{s}^{-1}$)
 432 1).

5.1.2 Isotopic records of surface water to precipitation

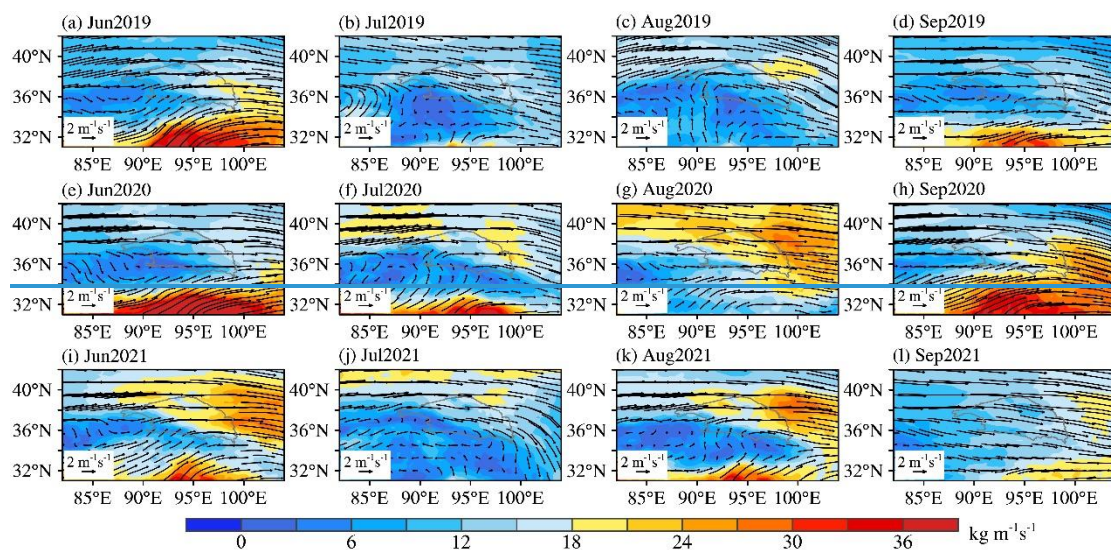
Owing to the scant sparse precipitation in the alpine arid region and its concentration in summer (June to September), the surface water isotopic characteristics records of surface water may mimic reflect local precipitation characteristics in the respective region during the wet season. The seasonal characteristics of stable H-O isotopes variation in the surface water, which consisted of enrichment during the wet season and depletion during the dry season (Figure 4); On a seasonal basis, the positive correlations between isotopic variations in surface water (Figure 3) isotopes and those of precipitation are extremely strong across most of the basin and its surrounding areas were consistent with the observed or simulated patterns of changes in precipitation isotopes in the basin and its surrounding areas within each year (Liu et al., 2009; Zhao et al., 2011; Gui-Juan et al., 2020; Wu et al., 2022). In particular, the $\delta^{18}\text{O}$ values at the sampling sites in the mountainous areas on the upper stream of each watershed were are positive higher during the wet season compared to the the dry season, which reflectsing the contribution input of precipitation with characterized by heavy isotopic signatures that is enriched in heavy isotopes to the river. Moreover, the mean $\delta^{18}\text{O}$ and δD values were are higher in watersheds (such as Qaidam and Bayin Rivers) during wet season, with correspondingly excessive rainfall greater precipitation (Figure S1). From this, it can be inferred that the river water stable H-O isotopes of each watershed in the basin were are primarily impacted predominantly influenced by summer precipitation during the wet season could be inferred. This is mostly because during largely due to the wet season coinciding with the rainy season, where the relatively more concentrated intensive rainfall events may can created directly form surface runoff and rapidly recharge the river.

In the Eastern Kunlun Mountains water system, the spatial trend of river water H-O isotopes depletion from west to east (Figure 4) elucidates the variation of precipitation isotopes in relation to the water vapor transport process, which can be attributed to the waning of westerly winds. Along the water vapor transport path, heavy isotopes are preferentially separated in precipitation formation, leading to an augmentation in the continental characteristics of water vapor carried by the air mass, while the precipitation formed by the remaining water vapor undergoes a gradual depletion of isotopes (Yang and Wang, 2020). Meanwhile, the two watersheds in the Qilian Mountains possess contrasting spatial variation characteristics relative to the Eastern Kunlun Mountains water system. Based on the comparison and analysis of the meteorological elements of Delingha and Da Qaidam (refer to Figure 2 for specific location) from 2010 to 2020, the average

464 annual precipitation of Delingha (276.36 mm) was 2.41 times higher than that of Da Qaidam
465 (114.79 mm), and the average annual temperature of Delingha (5.23 °C) was higher than that of
466 Da Qaidam (3.65 °C) by 1.58 °C. Since 1961, precipitation in the Bayin River has risen by as much
467 as 25.09 mm/10 a, which was more than six times greater than that of the Yuka River. Owing to
468 the abundance and marked magnitude of increase of precipitation, the seasonal $\delta^{18}\text{O}$ variation in
469 the Bayin River was approximately 1.79 times that of the Yuka River. Under similar conditions
470 where ice/snow meltwater recharge was present, the mean $\delta^{18}\text{O}$ and δD values of the Bayin River
471 were positively skewed by 1.52‰ and 7.26‰ relative to that of the Yuka River, respectively,
472 which can be attributed to the greater contribution of precipitation with heavy isotopic enrichment
473 characteristics to the river water. Therefore, the spatial and seasonal variations of the river water
474 H-O isotopes in the Qilian Mountains water system can be attributed to the variations in
475 hydrothermal condition and the varying extents of warming and humidification in the watershed.

476 To further explain the cause of seasonal and spatial variations of surface water $\delta^{18}\text{O}$ and δD
477 values, ERA5 reanalysis data in the rainy season (June to September) were used to calculate the
478 water vapor flux field in the Qaidam Basin and its surrounding areas and track the main paths of
479 the water vapor transport of precipitation (Hersbach et al., 2019). The results (Figure 6)
480 demonstrated that the water vapor path in and surrounding the basin is predominantly affected by
481 the mid-latitude westerly air masses (Yang and Wang, 2020) and the water vapor flux in the eastern
482 region of the basin is notably greater than that in the western region. This explains the spatial
483 change patterns of river water H-O isotopes (Figure 4) and hydrothermal conditions to a large
484 degree (Figure S1). The above findings are also supported by atmospheric and isotopic tracing
485 evidences. For example, the Tanggula Mountains (33°–35° N) form the physical and chemical
486 boundary of the Tibetan Plateau, and the northern region is fundamentally under the control of the
487 westerly wind, which hinders the South Asian monsoon from exerting a direct influence on the
488 Qaidam Basin (Yao et al., 2013; Kang et al. 2019; Wang et al., 2019). Furthermore, water vapor
489 source information can be reflected in d -excess, where the recycled moisture that evaporated under
490 conditions of low humidity and water carried by the westerly wind is considered to possess higher
491 d -excess values. The mean d -excess of basin river water samples during the wet season (11.45‰,
492 Table S1) was greater than 10‰, which reflects the characteristics of an alpine arid continental
493 climate and a water vapor source devoid of monsoon influences. In contrast, in the hinterland of
494 the Tibetan Plateau, south of the Tanggula Mountains, which is subject to considerable influences

495 from the South Asian monsoon circulation, the δ -excess values of summer precipitation and river
 496 water were in the range of 5‰–9‰, with mean value of 7‰ (Tian et al., 2001). The substantial
 497 differences in the δ -excess values between the two regions also support the above inference about
 498 the water vapor sources of the Qaidam Basin.



499
 500 **Figure 6.** Tropospheric water vapor flux from June to September 2019 to 2021 (below 500 hPa, unit: $\text{kg m}^{-1} \text{s}^{-1}$)

501 **5.1.3 Climate impact on isotopic spatial and temporal variation**

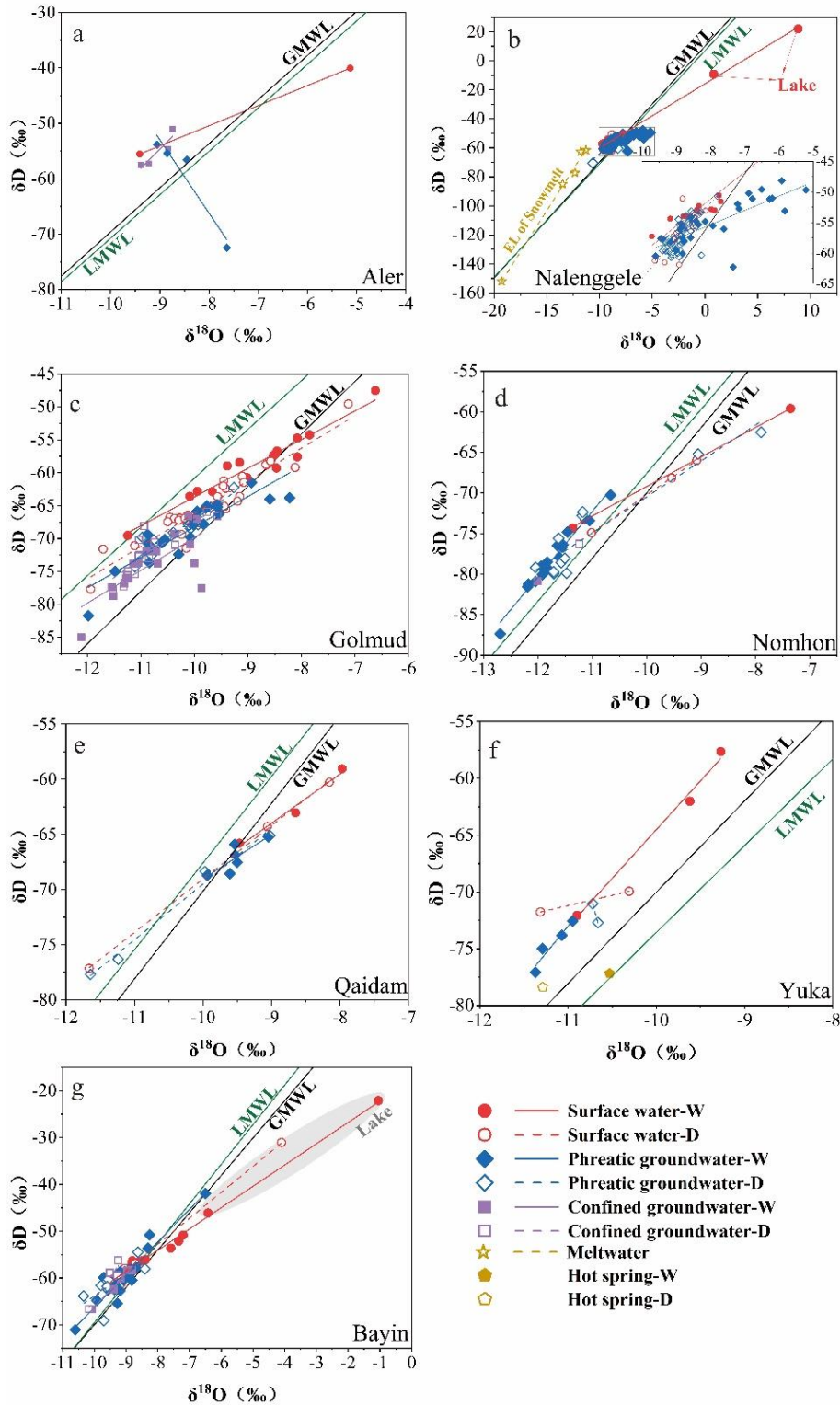
502 The spatial variation of surface water isotopes of the Eastern Kunlun Mountains water system
 503 depletion from west to east (Figure 3) reflects the variation of precipitation isotopes which are
 504 strongly influenced by westerlies moisture water vapor transportation transport. Heavy isotopes are
 505 preferentially separated in raindrops condensation along the westerlies trajectory, and long
 506 distance moisture advection leads to heavy isotope depleted precipitation due to rainout (Wang et
 507 al., 2016; Yang and Wang, 2020). Meanwhile, the isotope variations in the two watersheds in the
 508 Qilian Mountains are opposite to those in the Eastern Kunlun Mountains water system. Comparing
 509 the meteorological parameters of Delingha and Da Qaidam (refer to Figure S1 for specific location)
 510 from 2010 to 2020, the averagemean annual precipitation of Delingha (276.36 mm) was 2.41 times
 511 higher than that of Da Qaidam (114.79 mm), and the averagemean annual temperature of Delingha
 512 (5.23 °C) was 1.58 °C higher than that of Da Qaidam (3.65 °C). Precipitation in the Bayin River
 513 has increased by up to 25.09 mm per decade since 1961 (Figure S1). The seasonal $\delta^{18}\text{O}$ variation
 514 in the Bayin River is roughly 1.79 times that of the Yuka River, due to the marked increase in
 515 precipitation in Delingha. Under similar conditions of ice/snow meltwater recharge, the mean $\delta^{18}\text{O}$

516 and δD values of the Bayin River are higher than 1.52‰ and 7.3‰, respectively, relative to that
517 of the Yuka River, which can be attributed to a greater proportional contribution of precipitation
518 with heavy isotopic signatures to the river water. As a result, the change in river water isotopes in
519 the Qilian Mountains can be attributed to the differences in temperature and precipitation regimes,
520 as well as the extents of warming and humidification between the watersheds.

521 Given the ~~spatiotemporal~~ spatial and temporal variations ~~differences~~ of surface water $\delta^{18}O$ -
522 δD (Figure 43), samples ~~of from~~ different water bodies ~~in within~~ each watershed were incorporated
523 into the $\delta^{18}O$ - δD plot (Figure 7). The ~~presence of~~ considerable differences in the dual-isotopic
524 spectrum isotope distribution characteristics suggest ~~implies~~ that seasonal variations ~~changes~~ in the
525 surface water ~~H-O~~ isotopes in each watershed ~~water type~~ may be attributed ~~due~~ to
526 variability ~~differences~~ in the proportions of the contribution ratios of precipitation, ice/snow
527 meltwater, and groundwater throughout during both the wet and dry seasons. Hence, Equation 1 of
528 the MixSIAR model (Table 1) was employed to estimate the contribution of each potential
529 recharge endmember to ~~the river water~~ (Table 1). The findings reveal ~~indicated~~ that in the dry
530 season, groundwater discharge in mountainous areas maintains the base flow in each watershed
531 is maintained by the groundwater discharge in mountainous areas during the dry season, where
532 the with groundwater contribution of groundwater to base flow may reach up to 97% of the total
533 flow. Various proportions of precipitation, ice/snow meltwater and groundwater ~~During the wet~~
534 season, recharge the river water in each watershed is recharged by during the wet season ~~different~~
535 proportions of precipitation, ice/snow meltwater and groundwater. For example, in the area with
536 the most abundant ~~greatest~~ annual precipitation amount rainfall, the contribution of summer
537 precipitation to the Bayin River during the wet season may reach 84% ~~during the wet season~~. The
538 westerly water vapor forms more precipitation as a result of obstruction from landforms in the
539 eastern region of the basin, in contrast, as the source area of the Bayin River is in close proximity
540 to the eastern region of Qilian Mountains, although the summer monsoon is likened to ‘an arrow
541 at the end of its flight’ (a spent force), the latter continues to contribute more than 22% of the
542 oceanic water vapor to the nearby areas (Wu et al., 2022). The topographic obstruction and strong
543 convection form abundant precipitation, rendering the proportion of precipitation in the surface
544 runoff in the eastern basin region appreciably higher than that in other areas. Thus,
545 variability ~~differences~~ in the proportional contributions ~~proportions of contribution ratio~~ of each

546 recharge end-member during wet and dry seasons are the main factors responsible for the seasonal
547 variations in surface water isotopes in each watershed.

548 In summary, the ~~spatial patterns seasonal variations~~ and ~~seasonal variations spatial patterns~~
549 of surface water stable ~~H-O~~ isotopes are ~~caused by a consequence of~~ the ~~interaction~~ ~~combined~~
550 ~~effects~~ of ~~the extent of regional warming and humidification trends~~ ~~warmth and humidity in the~~
551 ~~region~~, ~~the~~ intensity of ~~the~~ mid-latitude ~~westerlies moisture transportation~~ ~~westerly wind water~~
552 ~~vapor transport~~, and local hydrometeorological conditions.



553

554 **Figure 7.** $\delta^{18}\text{O}$ - δD plots during dry wet seasons and in different water bodies in each watershed of the Qaidam
 555 Basin during dry and wet seasons—(W and D represent wet and dry seasons, respectively). Data source of
 556 LMWLs: a and b: Xu et al., 2017; c: this study; d and e: Xiao et al., 2017; f: Zhu et al., 2015; g: Tian et al., 2001.

557 **Table 1.** Contribution ratios of endmembers to river water during the wet and dry seasons based on $\delta^{18}\text{O}$ and
 558 d-excess (Unit: %; W and D represent wet season and dry season, respectively).

	Endmember	Groundwater	Meltwater	Tributary	Precipitation
Nalengele-W	Mean	0.41		0.47	0.12
	Max	0.60		0.74	0.13
	Min	0.18		0.27	0.08
	SD	0.12		0.13	0.02
Nalengele-D	Mean	0.90	0.10		
	Max	0.97	0.27		
	Min	0.73	0.03		
	SD	0.07	0.07		
Golmud-W	Mean	0.31	0.34	0.25	0.10
	Max	0.36	0.39	0.32	0.12
	Min	0.28	0.29	0.20	0.08
	SD	0.03	0.04	0.05	0.01
Golmud-D	Mean	0.32	0.25	0.42	
	Max	0.46	0.45	0.70	
	Min	0.19	0.11	0.21	
	SD	0.09	0.10	0.17	
Yuka-W	Mean	0.62	0.23		0.15
	Max	0.76	0.29		0.18
	Min	0.55	0.15		0.10
	SD	0.10	0.06		0.04
Bayin-W	Mean	0.26	0.04	0.25	0.45
	Max	0.35	0.05	0.43	0.84
	Min	0.08	0.02	0.06	0.23
	SD	0.08	0.01	0.11	0.19

559 5.2 Multi-sources of groundwater recharge and circulation mechanism
 560 Sources and spatial patterns of groundwater recharge

561 ~~The s~~Seasonal variations in groundwater aquifer H-O isotopes in each watershed suggests
 562 that ~~differences exist in~~ their recharge sources, forms, and rates fluctuate. The $\delta^{18}\text{O}$ - δD
 563 correlations~~relationships~~ of different seasons and ~~different~~ types of water samples can be used to
 564 ~~deduce~~elucidate the groundwater source compositions and recharge patterns. According to the
 565 seasonal variations in groundwater $\delta^{18}\text{O}$ - δD in each watershed (Figure 4) and the dual-isotopic
 566 spectrum of different water bodies within the watershed (Figure 7), The the Qaidam Basin
 567 groundwater systems can be ~~classified~~divided into three recharge types ~~of recharges according to~~
 568 ~~the seasonal changes in groundwater $\delta^{18}\text{O}$ - δD in each watershed (Figure 5) as well as the $\delta^{18}\text{O}$ -~~

569 ~~δD relationship of different water bodies within the watershed (Figure 7): modern precipitation~~
570 ~~and glacier snow melt water dominated recharge and fossil water as well.~~

571 5.2.1 ~~Heavy pP~~precipitation ~~in the wet season~~ -dominated recharge

572 In the Nalenggele River, which is situated in the southwestern basin, and the Qaidam and
573 Bayin Rivers in the eastern basin, groundwater $\delta^{18}\text{O}$ and δD values ~~were~~ are markedly positively
574 ~~skewed during the~~in wet season and negative in dry season (Figure 5). The groundwater isotope
575 data ~~distribution~~ in the majority of the wet seasons clusters near ~~was closer to~~ the LMWL and
576 GMWL compared to that during the dry season (Figures 7b, 7e, and 7g). ~~Moreover, indicating~~ the
577 isotopic signature ~~characteristics were~~ are similar ~~closer~~ to the river water and summer
578 precipitation in the same period (Table S1; Zhu et al., 2015), with different trends in evaporation
579 (Figures 7b, 7e and 7g). These results suggest ~~indicate the contribution of~~ precipitation recharge
580 ~~to~~ s groundwater during the wet seasons. The relatively significant ~~marked~~ seasonal variations of
581 H-O isotopes also demonstrates ~~show~~ that the aquifers in the eastern and southwestern Qaidam
582 Basin have a relatively rapid groundwater circulation ~~eyele~~ and present seasonal recharge. There is
583 an abundance and notable rise in precipitation ~~In in~~ the eastern basin; there is an abundance and
584 notable rise in precipitation ~~(Figure S1)~~. An interesting finding was that ~~which increased~~ ing
585 precipitation has directly caused ~~led to~~ a rise of 5 m in water level and an ~~surface~~ area expansion
586 of 1.59 times in a lake at ~~near~~ the headwaters ~~source~~ of the Nalenggele River in the southwestern
587 basin from 1995 to 2015 (Chen et al., 2019). The abundant Precipitation observed in the eastern
588 basin headwater ~~This further indicates the abundant precipitation in the headwater may~~ may also
589 be a potential source for the rapid seasonal recharge ~~of~~ groundwater recharge associated with the
590 rapid warming ~~climate~~ warming and humidification. Furthermore, ~~Additionally,~~ the tectonic
591 conditions of the recharge area are considered ~~believed to enhance~~ are ~~factors that are in favor of~~
592 driving seasonal groundwater recharge. The three watersheds coincide with collision zones of
593 intensive neotectonic movement, where a considerable number of deep faults and other volcanic
594 channels have developed within recharge areas (Figure 2; Tan et al., 2021). ~~These three watersheds~~
595 ~~happened to be situated in the collision zone (Figure 2), where neotectonic movement is strong,~~
596 ~~and there are substantial developments of deep fractures and faults in the recharge area.~~ It ~~t~~ can
597 be concluded ~~inferred from the aforementioned~~ that favorable hydrological and tectonic conditions
598 facilitate ~~promote~~ the formation of directly ~~and~~ rapid recharge ~~of~~ groundwater recharge ~~of~~

599 ~~precipitation and meltwater~~ through bedrock fissures ~~at high altitudes~~ under the large hydraulic
600 heads (>1000 m) ~~from precipitation and meltwater at higher altitudes~~, resulting in
601 ~~significant~~ substantial seasonal ~~variation~~ changes in the groundwater H-O isotopes in these regions
602 (~~Tan et al., 2021~~).

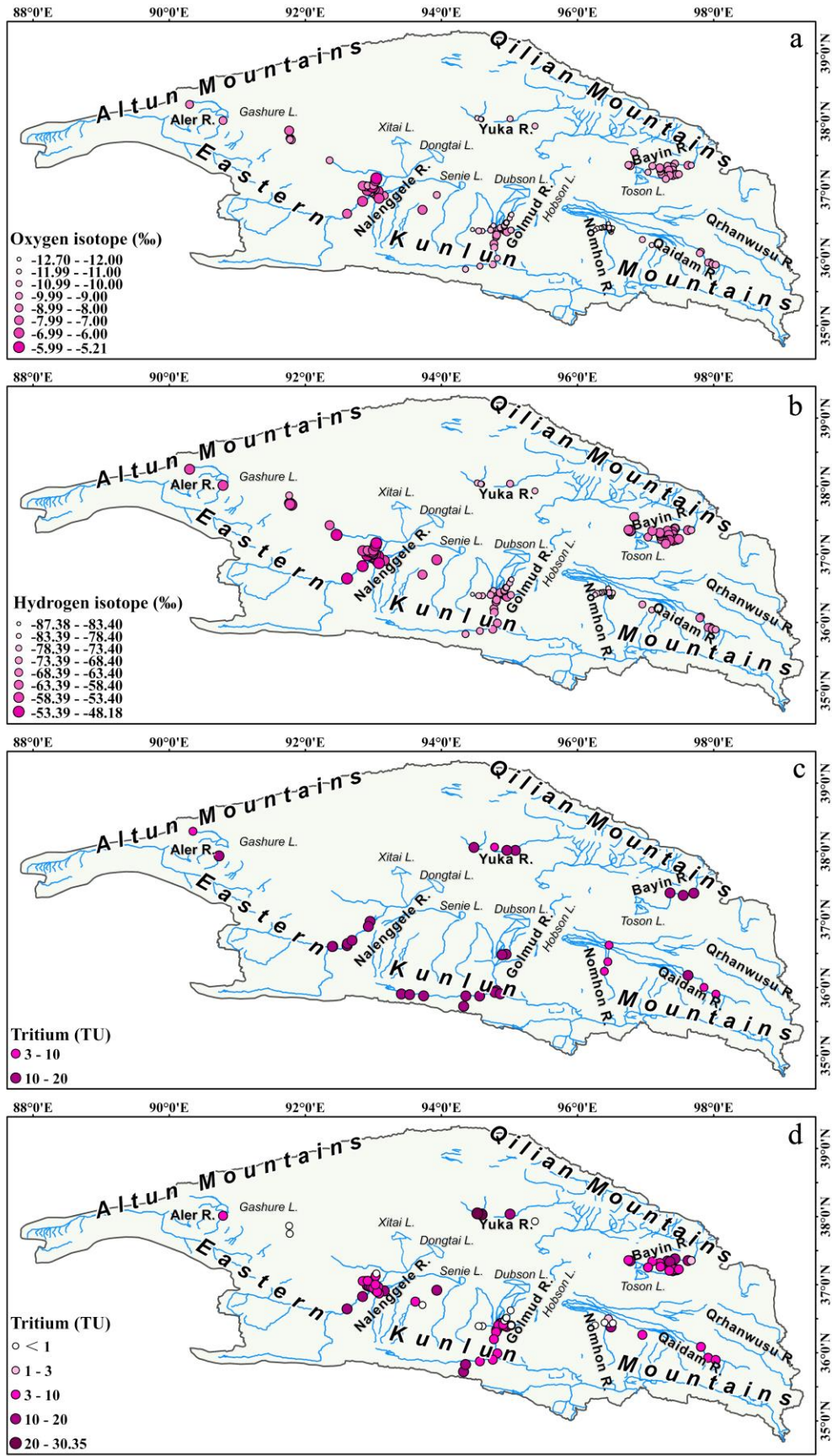
603 5.2.2 ~~Glacial~~ Glacier -snow melt water -dominated recharge

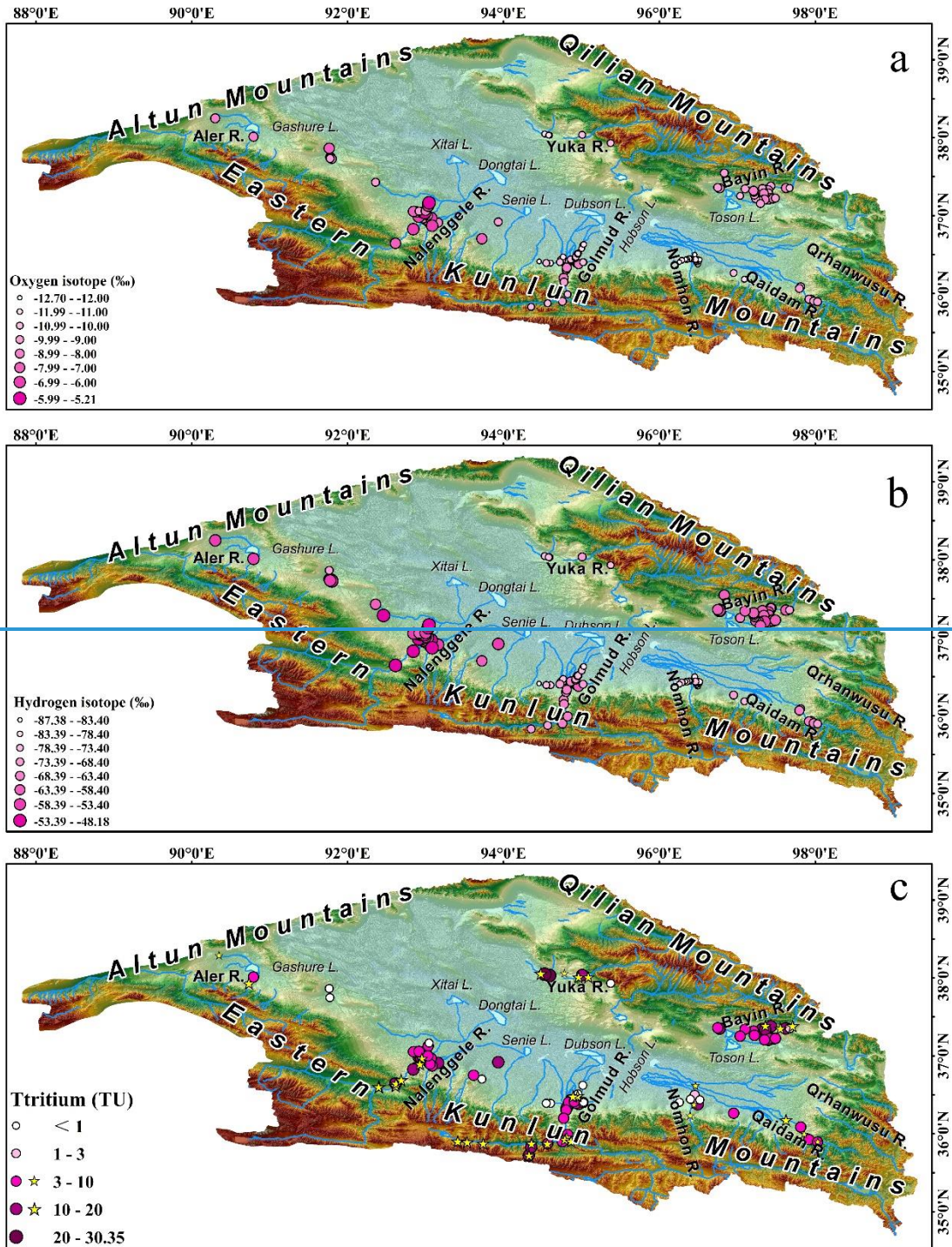
604 In the Nomhon and Yuka Rivers, ~~situated~~ located in the ~~central~~ middle region of the basin
605 region, groundwater H-O isotopes ~~were~~ are more depleted ~~during~~ in the wet season ~~compared~~
606 ~~to~~ than in the dry season (Table S1; Figure 54). ~~Figures 7d and 7f also show that the majority~~ Most
607 of the $\delta^{18}\text{O}$ - δD data for the groundwater samples in these two watersheds ~~were~~ are observed in the
608 lower left of the LMWL and GMWL (Figures 7d and 7f-), and ~~These~~ these values ~~were~~ far away
609 ~~from the LMWL and GMWL, and were~~ are more negative ~~more negatively skewed~~ relative to
610 river water, with characteristics ~~parallel~~ being closer to ~~the~~ those measured in snow-melt water
611 ~~obtained from~~ observed in the high-altitude Eastern Kunlun Mountain (Figure 35; Yang et al.,
612 2016). This ~~demonstrates~~ shows that the groundwater recharged by ice/snow meltwater ~~is~~ more
613 isotopically depleted ~~depleted in heavy isotopes~~, during both the wet- and dry seasons, ~~despite the~~
614 ~~fact that precipitation contributes less to the aquifer and the contribution of precipitation to the~~
615 ~~aquifer was relatively small. Similarly, non-monsoonal meltwater control of hydrological~~
616 ~~processes in monsoonal groundwater systems has also been observed on the eastern margin of the~~
617 ~~Tibetan Plateau~~ Similarly, on the eastern margin of the Tibetan Plateau, the phenomenon where
618 ~~the non-monsoon meltwater controls the monsoon groundwater system hydrological process has~~
619 ~~been observed~~ (Kong et al., 2019). The isotope signals ~~suggested~~ indicated that isotopically
620 depleted ice/snow meltwater ~~depleted in the heavy isotopes~~ in the source ~~region~~ area was released
621 ~~as a result of~~ due to elevated summer temperatures ~~the rising temperature in summer, and was~~
622 further depleted in the groundwater after mixing with groundwater recharged by seasonal
623 ~~meltwater and following the mixing of groundwater with the seasonal meltwater recharge, the~~
624 ~~groundwater was further depleted in heavy isotopes~~. Furthermore, owing ~~due~~ to the ~~scarce~~ low
625 precipitation in these two watersheds (61.39 and 121.78 mm, ~~respectively, Figure S1~~), ~~and that~~
626 ~~even~~ the fewer precipitation ~~events occurred~~ in 2020, ~~was even lower~~. Under extremely arid
627 ~~climate~~, the ~~seasonal~~ direct recharge to the aquifer from the limited precipitation was negligible ~~in~~
628 ~~this extremely arid climate. GRACE data also showed that the melting of solid water in the source~~

629 ~~area due to climate warming was a key factor driving the increase in the groundwater storage of~~
630 ~~the Qaidam Basin (Xiang et al., 2016). This further supports the inference that groundwater~~
631 ~~isotopic depletion during the wet season stems from the seasonal melting recharge of the~~
632 ~~eryosphere.~~

633 5.2.3 Fossil water -dominated recharge

634 In the Golmud River, the mean $\delta^{18}\text{O}$ value ~~during the wet season was is~~ 0.33‰ higher ~~during~~
635 ~~the wet season~~ than ~~that~~ during the dry season, ~~and with insignificant~~ seasonal changes ~~were not~~
636 ~~apparent~~, indicating ~~that the a limited share of seasonal groundwater recharge and a slow renewal~~
637 ~~rate proportion of seasonal groundwater recharge was small and the renewal rate was slow~~. The
638 ~~groundwater H-O isotope data of the groundwater lay mainly were mainly located~~ between the
639 LMWL and GMWL (Figure 7c), ~~indicating implying~~ that the ~~predominant main~~ recharge source
640 ~~was is different periods the atmospheric precipitation (Beyerle et al., 1998) seasons. Furthermore, In~~
641 ~~addition~~, the groundwater $\delta^{18}\text{O}$ and δD ~~values in the alluvial fan belt~~ exhibited a gradually
642 ~~decreased negatively skewed~~ trend along the flow path (Figures 8a and 8b). ~~For this watershed, A~~
643 ~~a prominent feature of this watershed~~ is the sizeable storage of confined groundwater, which is
644 ~~constantly continuously emanating discharging~~ at the front edge of the alluvial fan. Confined
645 groundwater $\delta^{18}\text{O}$ and δD values ~~are possesses more negative $\delta^{18}\text{O}$ and δD values that are more~~
646 ~~negative~~ than ~~those of~~ phreatic groundwater, and the mean $\delta^{18}\text{O}$ values ~~are similar during the wet~~
647 ~~and dry seasons, with minor seasonal variation (Table S1) during the wet dry seasons are~~
648 ~~consistent, without any seasonal changes. The substantial differences in isotopic characteristics~~
649 ~~between phreatic and confined groundwaters (Table S1) suggest that there are potential differences~~
650 ~~in their recharge sources. It is We hypothesizes speculated~~ that phreatic groundwater is
651 ~~predominantly~~ recharged ~~primarily~~ by ice/snow meltwater, while confined groundwater is slowly
652 and stably recharged and may be sustained by precipitation with low $\delta^{18}\text{O}$ and δD values or fossil
653 water formed ~~under during the~~ relatively cold ~~climatic conditions climate periods~~ (Xiao et al.,
654 2018). ~~This scenario is in fact observed in deep confined groundwater in many areas in the world~~
655 ~~(Ma et al., 2009; Jasechko et al., 2017).~~





657

658 **Figure 8.** Spatial distribution of groundwater $\delta^{18}\text{O}$ (a) and δD (b) in groundwater, and tritium concentrations
 659 in and surface water (c) and groundwater ^3H (ed) concentrations during the wet season. (Circle and asterisk
 660 represent groundwater and surface water, respectively)

5.3.2.4 Mechanism governing water cycle in alpine mountain-basin system
Water cycle mechanism

Being a direct constituent of water molecules, radioactive ^3H , tritium, with a half-life of 12.32 years, can be used to estimate the migration time of younger water. Particularly, in mixed water bodies consisting of younger water and fossil water, ^3H can be used to effectively characterize groundwater age and renewal rate in water bodies consisting of a mix of younger water and fossil water (Stewart et al., 2017; Xiao et al., 2018; Chatterjee et al., 2019; Shi et al., 2021). In accordance with the significant differences in $\delta^{18}\text{O}$ - δD of the various water bodies in each watershed (Figures 7, 8a, and 8b), the scale and extent of the groundwater recharge in the Qaidam Basin were further constrained/determined using the ^3H (Figures 8c and 8d) concentration. The spatial pattern of ^3H concentration spatial distribution pattern reveals/indicated that groundwater recharge rates varied significantly there were considerable differences in groundwater recharge rates at both intra- and inter-watershed scales (Figures 8c and 8d). Thus, the groundwater system was/is dominated by both regional and local recharge.

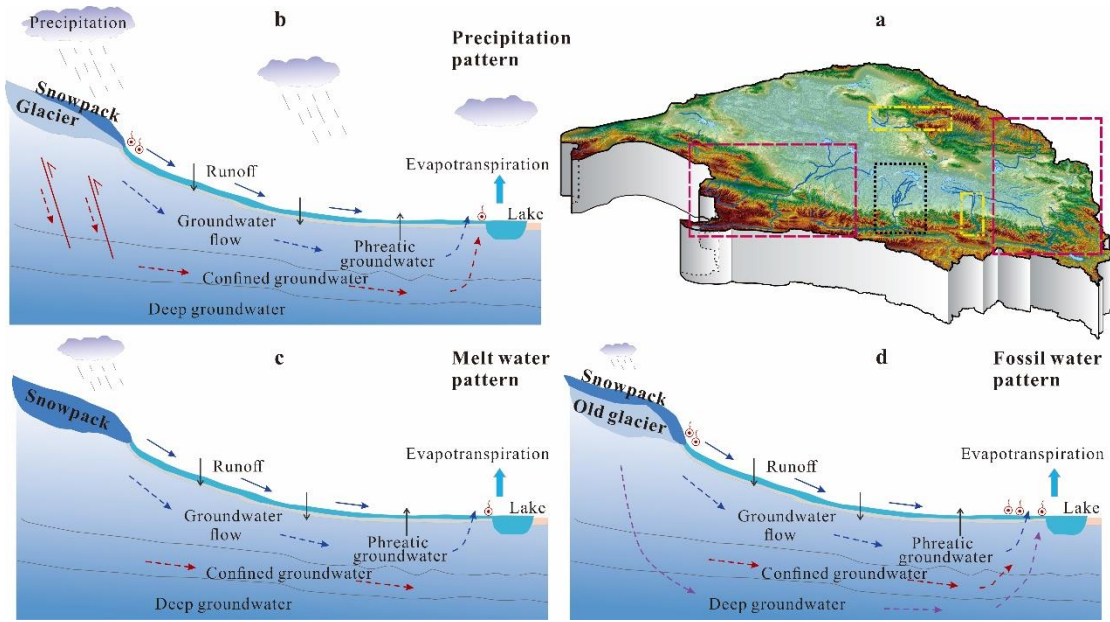
At the watershed scale, the ^3H concentration of the phreatic groundwater is significantly higher in alluvial fan areas in the alluvial fan zone near/along the river channel and mountain pass was considerably higher (Table S1; Figures 8c and 8d), and approximates/close to that of the river water. These results/This indicate/suggests that there is a close hydraulic connection/hydraulic interactions occurred between the surface water and groundwater, and that the aquifer also receives river water via/through vertical infiltration and lateral runoff/recharge. Hence, this portion of groundwater is therefore dominated by/seasonal/modern water recharge, which is younger, and has a relatively/rather rapid/more rapid renewal rate. The ^3H concentrations in the periphery of phreatic and confined groundwater ^3H concentrations at the edge of the alluvial fan were/are typically/largely below/less than 3 TU or lower than the detection limit, indicating that which ^3H is dead in comparison to was inconsistent with that near the river channel. These findings suggest that these aquifers are predominantly/mostly recharged by lateral runoff/flow, consisting primarily of sub-modern water (>60 years) or fossil water, with limited mixing of modern precipitation and seasonal meltwater, and a slow renewal rate, which consists largely of submodern water (>60 years) or fossil water, and the mixing proportion of modern precipitation

691 and seasonal meltwater is relatively low, with a slow renewal rate. This situation is especially
692 evident particularly apparent in Golmud and Nomhon Rivers (Liu et al., 2014; Cui et al., 2015;
693 Xiao et al., 2017, 2018), highlighting which also further reflects the importance of fossil water
694 content in recharging maintaining the aquifer in extremely arid regions.

695 At the basin scale, radioactive- ^3H data is concentration characteristics are consistent with the
696 water cycle information indicated by the seasonal variation changes in stable H-O isotopes.
697 Seasonal variations in $\delta^{18}\text{O}$ and δD values correspond to higher average ^3H concentration. In in the
698 phreatic groundwater systems situated in the eastern and southwestern basin regions, ^2H and ^{18}O
699 are relatively enriched during the wet season, ^3H has a relatively higher average concentration,
700 revealing that seasonal groundwater recharge is more significant noticeable, and that groundwater
701 age is overall younger (<60 years). Based on river seepage, modern meltwater and precipitation
702 may potentially also infiltrate through preferential flow paths favorable structural water passage
703 channels, such as fault zones developed on a large scale in the recharge area, resulting in resulting
704 in rapid aquifer recharge to the aquifer (Figure 9b; Tan et al., 2021). The contrary was observed in
705 the phreatic groundwater systems in of the western Qilian Mountains and central middle Eastern
706 Kunlun Mountains, were relatively depleted in ^2H and ^{18}O during the wet season, where the
707 depletion in heavy isotopes during wet season, accompanied by low the ^3H concentrations were
708 correspondingly low, and meant these aquifers systems were primarily mainly received recharged
709 from by seasonal ice/snow meltwater. In contrast However, the groundwater renewal rate was
710 relatively slow, owing to due to less and more the steady relatively stable meltwater recharge of
711 meltwater by comparison, the groundwater renewal rate was relatively slow (Figure 9c).

712 In confined groundwater, heavy H-O isotope depletion is greatest, with most samples having
713 very low ^3H concentrations (<3 TU), indicating a very slow recharge rate. The depletion of heavy
714 H-O isotope was greatest in confined groundwater, and the ^3H concentration of the majority of the
715 samples was very low (<3 TU) or fall below the detection limit, which indicates that the confined
716 groundwater recharge rate is very slow. Furthermore, most of the confined groundwater was
717 largely over over 100 years old and consisted mainly predominantly of submodern groundwater or
718 fossil water (Xiao et al., 2018). In the Golmud River, the effect of H-O isotope seasonal changes
719 in most of the confined groundwater was relatively small or showed almost no detectable change.
720 However, the confined groundwater in the discharge overflow zone continued to
721 discharge continued to spontaneously emanate after nearly a half a century of extraction mining,

722 and the ~~hydraulic water~~ pressure heads did not ~~decreased~~decrease, ~~which suggest~~implyings that
723 modern precipitation or ice/snow meltwater may recharges deep confined groundwater. Some
724 confined groundwaters possess ~~discernible~~recognizable seasonal isotopic ~~seasonal~~ effects, and the
725 existence of a certain proportion of ongoing ~~continuous~~ recharge, even on a seasonal scale, cannot
726 be ~~excluded~~ruled out. ~~In addition,~~ large karst springs have also developed in the mountainous
727 areas of ~~the~~ Golmud River. ~~Moreover, a large karst spring (KLSQ-1) was observed near the~~
728 ~~mountain pass, with a flow rate as high as 224.7 L/s. In mountainous areas, w~~Well-formed karst
729 ~~cavities caves~~ and fissures provide conduits ~~to enable the~~for direct ~~infiltration of~~ precipitation or
730 meltwater infiltration. ~~Following~~With deep circulation, precipitation and meltwater generate
731 regional subsurface flow that recharges the confined groundwater in the overflow zone in the long
732 term, allowing continuous flow under a ~~precipitation and meltwater give rise to regional subsurface~~
733 ~~runoff, which recharges confined groundwater in the overflow zone over a long distance, thus~~
734 ~~causing it to flow continuously under the effect of a large hydraulic head (approximately about~~
735 1,000 m) (Figure 9d). Moreover, the H-O isotopic signals of confined groundwater in part of the
736 alluvial fan front in the Golmud and Bayin Rivers, ~~the H-O isotopic signals of some confined~~
737 ~~groundwaters at the front edge of the alluvial fan were~~are largely similar~~essentially consistent~~ with
738 ~~that those~~ of the nearby phreatic groundwater, ~~and the~~with ³H concentrations ~~was~~ close to 10 TU.
739 These findings also suggest that confined groundwater recharge may have occurred through
740 aquitard or by leakage recharge in nearby skylights.~~the confined groundwater may pass through~~
741 ~~the aquitard or leakage recharge occurs in the local skylights.~~



742

743 **Figure 9.** Schematic diagram of the Qaidam Basin water cycle model (b represents the ~~purple~~ dashed box;
 744 c represents the yellow dashed box; and d represents the black dashed box).

745 5.4-3 Isotope hydrology responses to climate change and indication of water cycle trends ~~under~~
 746 climate change

747 ~~Since the 1980s,~~ The Qaidam Basin has experienced rapid warming at a rate more than twice
 748 ~~of~~ the global average ~~since the 1980s~~ (Wang et al., 2014; Kuang and Jiao, 2016; Yao et al., 2022).
 749 Since ~~1960~~1961, the 10- and 30-year mean temperature and precipitation average annual
 750 temperature and precipitation variations ~~changes~~ and increasing rising rates ~~over every 10 and 30~~
 751 years at eight meteorological stations in the basin (Figure 10a) have and continuous air temperature
 752 and precipitation change trends at two representative meteorological stations in the north and south
 753 (Delingha and Golmud) (Figure 10b) have demonstrated ~~shown~~ that the current present warming
 754 and humidification trends in the this northeastern Tibetan Plateau basin, northeastern Tibetan
 755 Plateau, are continuously strengthening ~~are continuously strengthening~~ (Figure 10). Changes in
 756 surface water and groundwater isotopes in the Qaidam Basin reflect different sensitivities to
 757 climate change at both seasonal and multi-year scales. Previously, it was assumed ~~the general~~
 758 assumptions were that the isotopic composition of the surface water and groundwater systems did
 759 not vary with time, at least on interannual intervals ~~scales~~, and was relatively rather stable (Boutt
 760 et al., 2019). However, isotopic variability in water bodies over the past 40 years, ~~the isotopic~~
 761 variations of water bodies have demonstrated ~~suggests~~ that there is a variable degree of interannual

762 variability in surface water and groundwater isotopes, with interannual variability in mean $\delta^{18}\text{O}$
763 values greater than 3‰ (Figure 11). ~~varying degrees of interannual differences in surface water~~
764 ~~and groundwater isotopes exist and interannual variations in the average $\delta^{18}\text{O}$ value are greater~~
765 ~~than 3‰ (Figure 11). Therefore, isotopic changes reflect different extents of sensitivity to climate~~
766 ~~change, regardless of the seasonal or multi-year scale.~~ The spatiotemporal spatial and temporal
767 variability of isotopic signals can be ascribed to differences in the extent of warming and
768 humidification across the basins in each watershed. Wang et al. (2014) highlighted that while the
769 Qaidam Basin has experienced rapid warming ~~in over~~ the past 50 years, ~~the extent of~~ warming and
770 humidification have been markedly asynchronous in different regions in different regions is
771 ~~noticeably not in synch, where the with~~ rates of temperature ~~increase rise~~ ranged from 0.31 to
772 0.89 °C ~~per decade/10a~~ and the ~~rates of rate of~~ rainfall ~~increase increase~~ ranged from 1.77 to 25.09
773 mm ~~per decade/10a~~ (Figure S1). ~~The correlation between $\delta^{18}\text{O}$ of watershed surface groundwater~~
774 ~~and temperature and precipitation showed (Figure 12) that the multi-year scale $\delta^{18}\text{O}$ variations in~~
775 ~~the basin surface water and groundwater had a more significant positive correlation with~~
776 ~~precipitation in the same period than temperature (Figures 12b and 12d).~~ It is noteworthy that Of
777 note, surface water ~~was is~~ more ~~responsivesensitive~~ to precipitation ~~(Figures 12a and 12b)~~,
778 ~~whereas while~~ groundwater ~~was is~~ more sensitive to temperature ~~(Figures Figure 12) 12a and 12c~~.
779 This phenomenon suggests that ~~the rise in increased precipitation rainfall~~ may ~~influence affect~~ the
780 water cycle by promoting slope runoff and groundwater infiltration in mountainous ~~regions areas,~~
781 ~~and indicates that the~~ warming will ~~lead to cause~~ the ~~ablation of~~ solid water ablation at higher
782 ~~elevations altitudes to thereby accelerate accelerating the~~ groundwater recharge ~~of to~~ aquifers
783 through bedrock fissures. In addition, elegant The GRACE and remote sensing monitoring findings
784 ~~suggested also demonstrated~~ that the increase in terrestrial water storage in the Qaidam Basin was
785 strongly correlated with increased is closely linked to the rise in precipitation rainfall and glacier
786 meltwater recharge (Song et al., 2014; Jiao et al., 2015; Xiang et al., 2016; Wei et al., 2021; Zou
787 et al., 2022), which fully supported ~~eds~~ the isotope-based conjecture. Furthermore, a recent study
788 found research demonstrates that the accelerated conversion of ice and snow ~~on the Tibetan Plateau~~
789 into liquid water on the Tibetan Plateau has led to an imbalance in the “Asia Water Tower”, with
790 the Qaidam Basin being one of the ~~major regions experiencing an key regions increase in~~ where
791 liquid water has grown (Yao et al., 2022). ~~The consistency of data on H-O The~~ isotopes, remote
792 sensing and hydrometeorology data are consistent with the observation shows that the Qaidam

793 Basin is the most rapid and substantial warming a region in the Tibetan Plateau ~~with the most rapid~~
794 ~~and substantial warming~~. Global warming affects the basin by redistributing causing a
795 ~~redistribution of~~ precipitation and melting ice and snow in high elevations altitude areas, resulting
796 in ~~a rise in~~ groundwater storage increase and ~~an lakes expansion of the area of lakes, among other~~
797 ~~effects. Additionally, the corresponding rise in precipitation in the mountainous areas is able to~~
798 ~~supplement the rapidly melting ice and snow to a certain degree. This~~ The trend of increasing water
799 storage ~~increase~~ in the Qaidam Basin is likely to continue in the 21st century. The highly coupled
800 results findings of different observation methods further emphasize the sensitivity and potential of
801 water ~~stable~~ isotopes in tracing water cycles and climate change.

802 ~~Due to~~ Under the influence effects of climate change and the intensive intensification of
803 cryosphere retreat, runoff has changed considerably dramatically on the Tibetan Plateau, which
804 with significant effects on drastically impacted the spatiotemporal spatial and temporal distribution
805 ~~of~~ water resources distribution (Wang et al., 2021). ~~Based on our observation results, it can be~~
806 ~~speculated that with continued rapid warming and humidification, the water resources of the~~
807 ~~watershed with substantial seasonal recharge may manifest as follows:~~ The rapid changes in water
808 resources in the Qaidam Basin are likely because:

809 1) ~~The amount of~~ The surface water and groundwater resources will considerably increase
810 significantly in the short term (in recent decades) ~~due to continued rapid warming and~~
811 ~~wetting because of the shift of snow line and rapid melting of ice and snow coupled with the~~
812 ~~increase in precipitation~~. For example, water storage in the Bayin and Qaidam Rivers in the
813 eastern basin is likely to continue to increase with a high renewal capacity in the long term
814 under the influence of sustained climate change and the abundant and significantly
815 increasing precipitation as a result of the abundant and marked increase in precipitation and
816 strong water resource renewal capability, the water reserves may sustain an increasing trend
817 ~~in the long term under the influence of continuous climate warming~~. This phenomenon has
818 been verified in many regions of the Tibetan Plateau ~~and as well as~~ some alpine watersheds
819 in high-latitude Switzerland (Xiang et al., 2016; Malard et al., 2016; Shi et al., 2021).

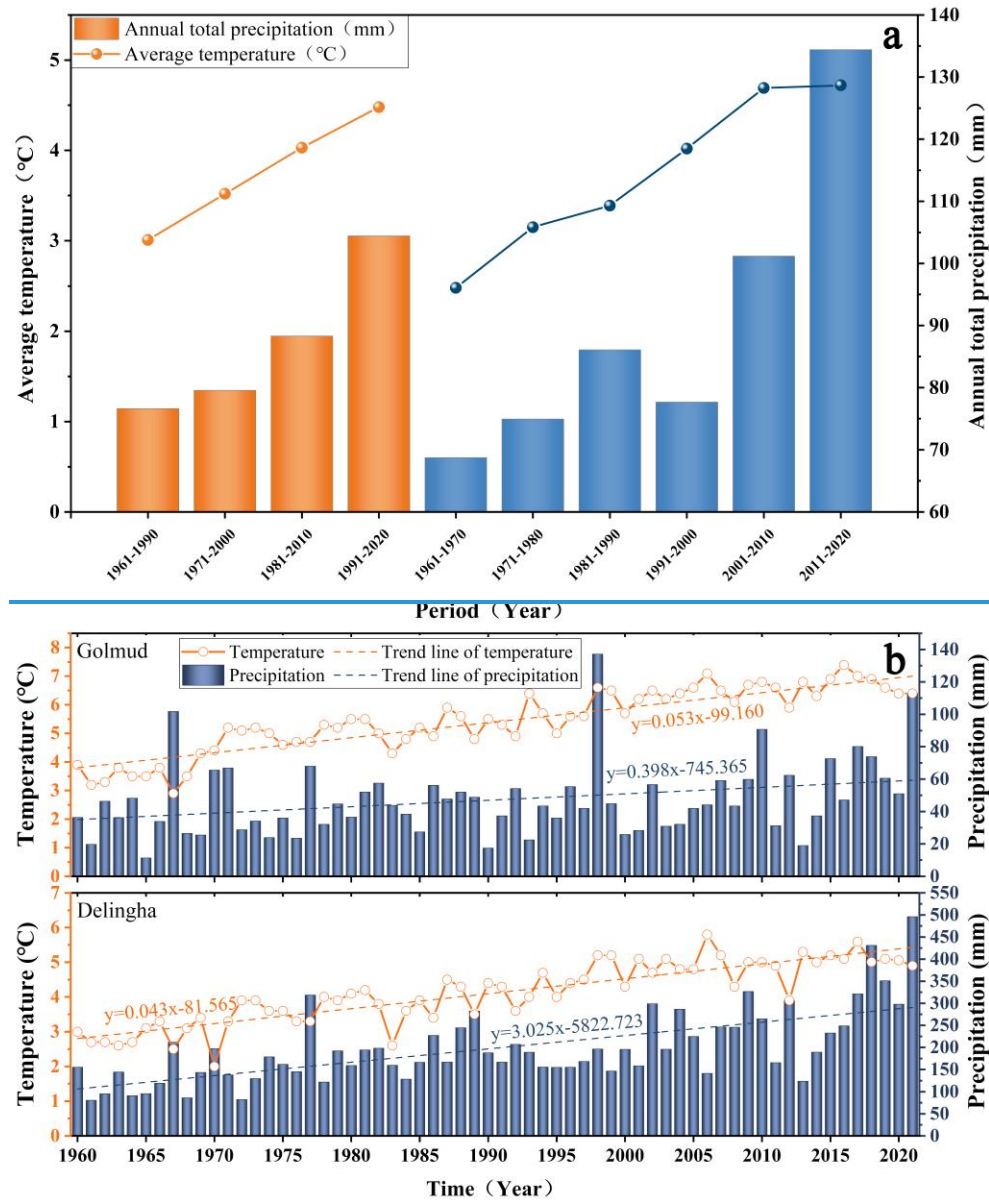
820 ~~Moreover, t2)~~ The decadal scale climatic oscillation cyclical nature of climate change also
821 suggests that the massive shrinking cryosphere cryosphere retreat on a large scale may not
822 sustain surface be sustainable for watershed surface water and groundwater recharge in the

823 basin (Wang et al., 2023). It is expected that water resources in the southwestern basin (e.g.,
824 Nalenggele River) may continue to increase for a certain period followed by a large-scale
825 decrease under future climate change scenarios. This is a general trend that has occurred in
826 the Tibetan Plateau as well as regions around the world with large-scale glacial coverage
827 area in alpine watersheds. ~~It was reported that the glaciers~~ Glaciers in the southwestern basin
828 are reported to be continuously losing mass regularly (-0.2 to -0.5 m/a), a trend that and
829 ~~this trend has substantially~~ has increased substantially from 2018 to 2020,
830 notably particularly in-at the headwaters of Nalenggele River, where ~~the~~ glacier elevation
831 has been reduced by 5.42 m since 2000 (Shen et al., 2022). However, ~~as a result of the low~~
832 ~~precipitation in the southwestern basin, completing achieving~~ the hydrologic
833 ~~budget equilibrium in recharge will remains remain~~ a challenge given strong decoupling
834 ~~between the~~ rapid melting of ice and snow caused by ~~climate~~ warming versus scarce
835 precipitation in the southwestern basin, even if precipitation continuously continues to
836 increases in the future.

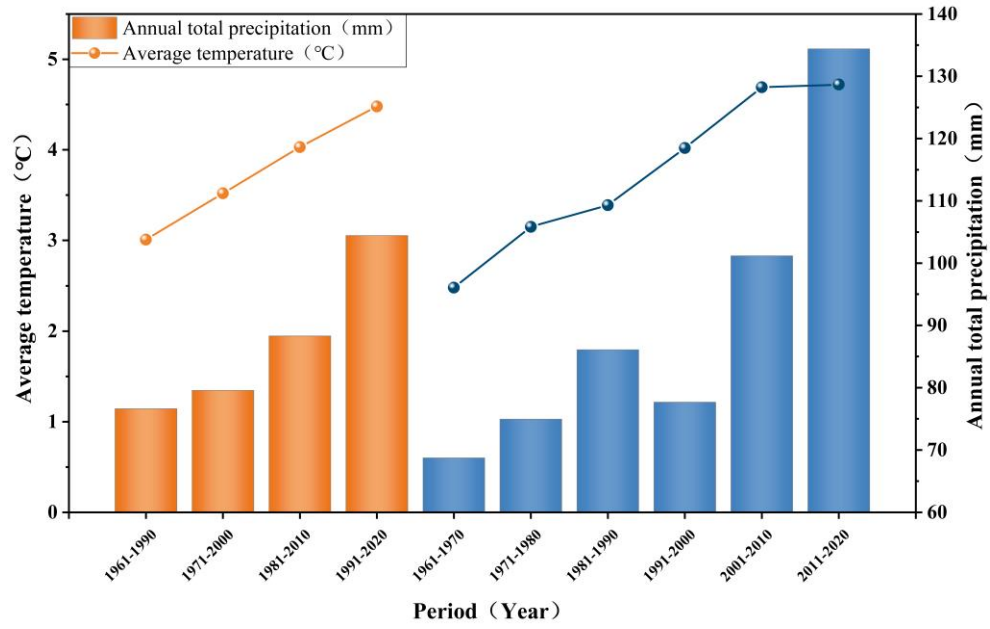
837 ~~This means that in the future climate change scenario, water resources in the southwestern~~
838 ~~basin watershed (such as Nalenggele River) may continue to rise for a certain period before~~
839 ~~showing a large scale decrease. This trend of initial increase followed by decrease is~~
840 ~~common in the Tibetan Plateau or regions with relatively little precipitation in alpine~~
841 ~~watersheds around the world. Furthermore,~~ 3) in-In the watersheds of the central middle
842 basin (Nomhon, Golmud, and Yuka Rivers), there is a long-term large-scale groundwater
843 mining during the agriculture and industry development, accompanied by strong local
844 evaporation. while ~~The sparse precipitation in the source area led to a melt dependence,~~
845 although the surface ~~water and groundwater recharge here is-are~~ relatively stable,

846 ~~the long term large scale exploitation of groundwater in these three areas during the industrial~~
847 ~~and agricultural development processes has decreased the precipitation in the source area~~
848 ~~and led to a reliance on ice and snow melting. Moreover,~~ 4) a Future decline in groundwater
849 level ~~fluctuations in the future is dropping seems to be inevitable in the basin with glacier~~
850 retreat and reducing of melt water in the mountainous source area. Data monitoring
851 Monitoring of the data from five shallow groundwater boreholes ~~in-along~~ the alluvial fan
852 belt of the Golmud River ~~showed shows~~ that ~~the~~ groundwater levels has-have fluctuated
853 since 2011, and reduced declining by an average of -1.18 m/a ~~since 2011~~ (Figure S2).

854 Therefore, ~~Whether-whether~~ the ~~enhanced-increase-in~~ water resource renewal capacity and
 855 water storage in the Qaidam Basin can ~~remain-stay~~ stable ~~in the future~~ is a scientific issue
 856 ~~that is worthy of considering-consideration in the future.~~

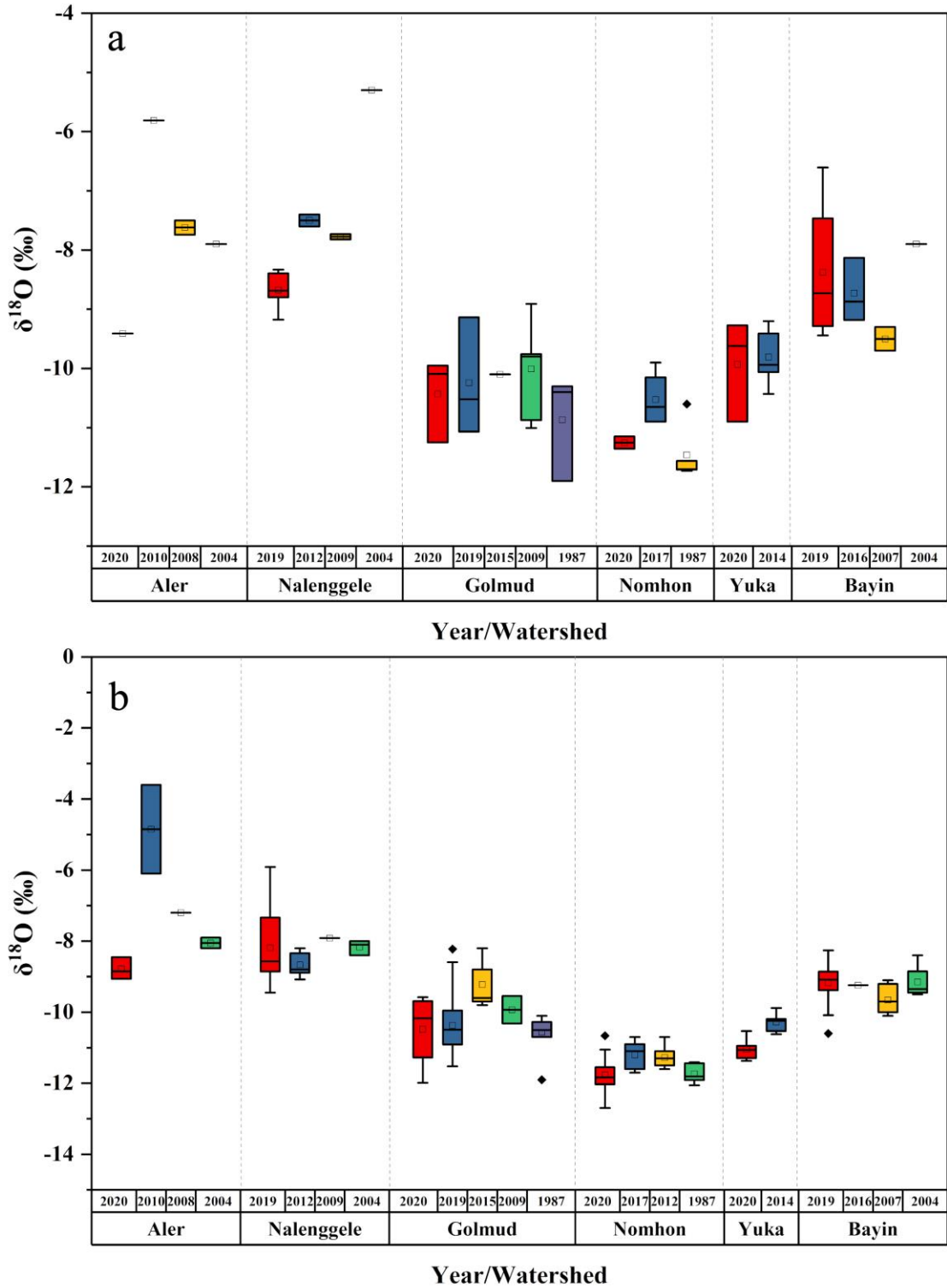


857



858

859 **Figure 10.** Average temperature and precipitation in the Qaidam Basin every 30 years and 10 years from 1960
 860 1961 to 2020. (a); interannual changes in temperature and precipitation at the Golmud and Delingha
 861 meteorological stations (b)



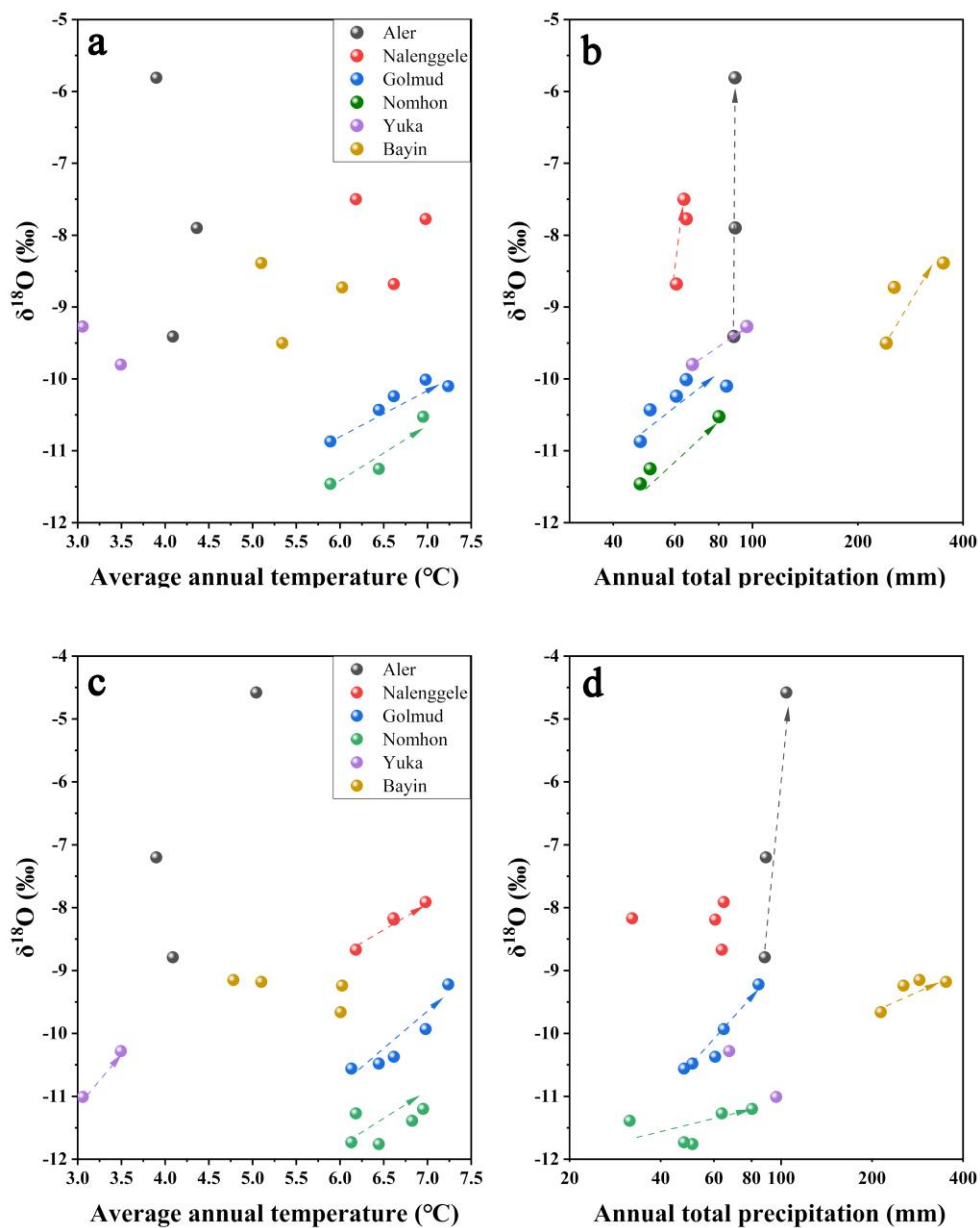
862

863 **Figure 11.** Interannual variations in the river water (a) and groundwater (b) $\delta^{18}\text{O}$ in the Qaidam Basin.

864 (Date source: Aler: 2004, Wang et al., 2008; 2008, Tan et al., 2009; 2010, Ye et al., 2015. Nalenggele: 2004,

865 Wang et al., 2008; 2009, Tan et al., 2012; 2012, Xu et al., 2017. Golmud: 1987, Wang et al., 2008; 2009,

866 [Tan et al., 2012; 2015, Xiao et al., 2018. Nomhon: 1987, Wang et al., 2008; 2012, Cui et al., 2015; 2017,](#)
867 [Zhao et al., 2018. Yuka: 2014, Zhu, 2015. Bayin: 2004, Wang et al., 2008; 2007, He et al., 2016; 2016,](#)
868 [Wen et al., 2018.\)](#)



869
870 **Figure 12.** Surface water $\delta^{18}\text{O}$ and temperature (a) and precipitation (b); Groundwater $\delta^{18}\text{O}$ and temperature (c)
871 and precipitation (d) in the Qaidam Basin. –(The light lines indicate $\delta^{18}\text{O}$ change with temperature and
872 precipitation.)

873 **6. Conclusion**

874 (1) ~~The contribution of precipitation and ice/snow meltwater is the main factor that drives the~~
875 ~~accelerated water cycle in the Qaidam Basin. The spatiotemporal spatial and temporal~~ variations
876 of $\delta^{18}\text{O}$ and δD in surface water and groundwater $\delta^{18}\text{O}$ and δD ~~in~~of the Qaidam Basin reflect their
877 dynamic hydrological responses to climate change, water sources, ~~climate warming~~, and local
878 temperature and precipitation regimes~~neotectonic movements~~, especially precipitation, at
879 interannual and seasonal scales.

880 (2) The mean values of surface water $\delta^{18}\text{O}$ and δD in the Eastern Kunlun Mountains
881 gradually decrease eastward, whereas the opposite is true for the Qilian Mountains river system,
882 reflecting the intensity of westerlies moisture transport and the influence of local climatic
883 conditions, respectively. Surface water H-O isotopes are enriched during the wet season and
884 relatively depleted during the dry season with a remarkable evaporation effect. The mean values
885 of surface water $\delta^{18}\text{O}$ and δD in the Eastern Kunlun Mountains water system are gradually
886 decreased negatively skewed from west to east, and the reverse holds true for the Qilian Mountains
887 water system. Surface water is enriched in heavy H-O isotopes during the wet season and is
888 relatively depleted during the dry season. The base flow is maintained by groundwater recharge
889 during the dry season, and while receiving varying proportions of groundwater (26%–62%),
890 ice/snow meltwater (23%–47%) and precipitation (10%–45%) are received during the wet season.
891 The seasonal isotopic variability ~~is~~differences of isotope are determined by the quantity of
892 precipitation level and its gradient increase in the watershed basin, with precipitation in the Qilian
893 Mountains contributing more to rivers than in the eastern Kunlun Mountains, and the spatial
894 change patterns reflect the influence of water vapor transport intensity of the westerly path and
895 local climatic conditions. The base flow is maintained by groundwater recharge during the dry
896 season, and varying proportions of groundwater (26%–62%), ice/snow meltwater (23%–47%) and
897 precipitation (10%–45%) are received during the wet season. The contribution of precipitation to
898 surface rivers in the Qilian Mountains is greater than that of the Eastern Kunlun Mountains.

899 (2) The key factor accelerating groundwater circulation in the Qaidam Basin is the
900 contribution of precipitation and meltwater produced by climate change. The phreatic groundwater
901 systems located in the collision and convergent convergence zone of different several mountain
902 ranges is are distinguished~~characterized~~ by enriched H-O isotopes during wet season, high

903 ~~concentrations of radioactive~~³H ~~concentrations~~, and marked rapid seasonal recharge ~~during the~~
904 ~~wet season~~. Modern precipitation meltwater and meltwater precipitation ~~are able to can~~ infiltrate
905 through favorable structural conduits (e.g., large-scale active fault zones) ~~water channel passages,~~
906 ~~such as large-scale active fault zones, giving rise to~~resulting in rapid groundwater recharge. In
907 contrast, the ~~phreatic~~ groundwater systems in the western ~~region of the~~ Qilian Mountains and the
908 ~~central-middle region of~~ Eastern Kunlun Mountains ~~have are~~ depleted in H-O isotopes during wet
909 season and ~~low~~³H concentrations are low ~~during the wet season~~, and ~~they are~~ primarily~~mainly~~
910 slowly recharged by seasonal ice/snow meltwater, which consisted ~~which consists~~ of modern water
911 and submodern water (>60 years) ~~maintained together~~. The confined groundwater is considerably
912 depleted in H-O isotopes, and for the most part exhibits imperceptible ~~a majority has no apparent~~
913 seasonal changes. ~~The~~³H concentrations is are very low ~~or below the detection limit~~, and ~~the~~
914 recharge is quite relatively slow, dominated by~~with~~ fossil water ~~dominated~~.

915 (3) Warming climate ~~Climate warming~~ has exerted a substantial impact on the hydrological
916 processes across~~throughout~~ the ~~whole~~ basin, accelerating~~thereby driving~~ water cycle acceleration
917 and raising~~increases in~~ water storage uncertainties~~fluctuations~~ in the eastern and southwestern
918 basin ~~regions via through~~ the increase ~~in~~ precipitation and melting of glaciers and snow. However,
919 this increasing trend of water resources in the basin seems to be unsustainable. ~~the cyclical nature~~
920 ~~of climate change suggests that this trend is unsustainable. As precipitation increases and solid~~
921 ~~water ablation in mountainous regions becomes severely out of balance, t~~The southwestern basin
922 may could suffer~~face~~ a rapid decline~~loss~~ in total water resources in the future as precipitation
923 increases and solid water ablation in mountainous areas becoming severely out of balance
924 undergone climatic extreme changes.

925

926

927 **Author Contribution**

928 Conceptualization: Yu Zhang, Hongbing Tan; Funding acquisition: Xiyang Zhang;
929 Investigation: Peixin Cong; Resources: Wenbo Rao; Visualization: Dongping Shi; Writing–
930 original draft: Yu Zhang; Writing–review & editing: Hongbing Tan.

931 **Acknowledgments**

932 This study was financially supported by the National Natural Science Foundation of China
933 (U22A20573), [the Fundamental Research Funds for the Central Universities \(B230205010\)](#), and
934 the Postgraduate Research & Practice Innovation Program of Jiangsu Province (KYCX22_0666).
935 [We thank the editors, Prof. Michael K. Stewart and the other two anonymous reviewers for](#)
936 [providing a list of critical and very valuable comments that helped to improve the manuscript. We](#)
937 [also thank Prof. Beckie, R. D. for writing suggestions and thoughtful reviews with the final](#)
938 [revision.](#) We would like to express our gratitude for all members' help both in the field observation
939 and geochemical analysis in the laboratory.

940 **Declaration of interests**

941 The authors declare that they have no known competing financial interests or personal
942 relationships that could have appeared to influence the work reported in this paper.

943 **Data Availability Statement**

944 The complete list of isotopes and their values is available in Table S1 in Supporting
945 Information. The meteorological data can be obtained on China Meteorological Data Network
946 (<http://data.cma.cn>). The monthly mean ERA5 reanalysis data ($0.25^\circ \times 0.25^\circ$) can be obtained from
947 European Centre for Medium-Range Weather Forecasts (ECMWF, <https://www.ecmwf.int/>).

948 **References**

- 949 Ahmed, M., Chen, Y., & Khalil, MM (2022). Isotopic Composition of Groundwater Resources in
950 Arid Environments. *Journal of Hydrology*, 127773.
- 951 Bam, EK, Ireson, AM, van Der Kamp, G., & Hendry, JM (2020). Ephemeral ponds: Are they the
952 dominant source of depression-focused groundwater recharge?. *Water Resources Research*,
953 56(3), e2019WR026640.
- 954 Befus, KM, Jasechko, S., Luijendijk, E., Gleeson, T., & Bayani Cardenas, M. (2017). The rapid
955 yet uneven turnover of Earth's groundwater. *Geophysical Research Letters*, 44(11), 5511-
956 5520.
- 957 [Benettin, P., Rodriguez, N. B., Sprenger, M., Kim, M., Klaus, J., Harman, C. J., ... & McDonnell,](#)
958 [J. J. \(2022\). Transit time estimation in catchments: Recent developments and future directions.](#)
959 [Water Resources Research](#), 58(11), e2022WR033096.

960 [Beyerle, U., Purtschert, R., Aeschbach-Hertig, W., Imboden, D. M., Loosli, H. H., Wieler, R., &](#)
961 [Kipfer, R. \(1998\). Climate and groundwater recharge during the last glaciation in an ice-](#)
962 [covered region. *Science*, 282\(5389\), 731-734.](#)

963 Boutt DF, Mabee SB, Yu Q. Multiyear increase in the stable isotopic composition of stream water
964 from groundwater recharge due to extreme precipitation[J]. *Geophysical Research Letters*,
965 2019, 46(10): 5323-5330.

966 Bowen, GJ, Cai, Z., Fiorella, RP, & Putman, AL (2019). Isotopes in the water cycle: regional-to
967 global-scale patterns and applications. *Annual Review of Earth and Planetary Sciences*, 47(1).

968 Chang, Q., Ma, R., Sun, Z., Zhou, A., Hu, Y., & Liu, Y. (2018). Using isotopic and geochemical
969 tracers to determine the contribution of glacier-snow meltwater to streamflow in a partly
970 glacierized alpine-gorge catchment in northeastern Qinghai-Tibet Plateau. *Journal of*
971 *Geophysical Research: Atmospheres*, 123(18), 10-037.

972 Chatterjee, S., Gusyev, MA, Sinha, UK, Mohokar, HV, & Dash, A. (2019). Understanding water
973 circulation with tritium tracer in the Tural-Rajwadi geothermal area, India. *Applied*
974 *Geochemistry*, 109, 104373.

975 Chen, C., Zhang, X., Lu, H., Jin, L., Du, Y., & Chen, F. (2021). Increasing summer precipitation
976 in arid Central Asia linked to the weakening of the East Asian summer monsoon in the recent
977 decades. *International Journal of Climatology*, 41(2), 1024-1038.

978 Chen, J., Wang Y., Zheng, J., & Cao L. (2019). The changes in the water volume of Ayakekumu
979 Lake based on satellite remote sensing data. *Journal of Natural Resources*, 34(6), 1331- 1344
980 (in Chinese with English abstract)-.

981 [Clark, I. D., & Fritz, P. \(2013\). *Environmental isotopes in hydrogeology*. CRC press.](#)

982 Condon, LE, Atchley, AL, & Maxwell, RM (2020). Evapotranspiration depletes groundwater
983 under warming over the contiguous United States. *Nature communications*, 11(1), 1-8.

984 Craig, H. (1961). Isotopic variations in meteoric waters. *Science*, 133(3465), 1702-1703.

985 Cui, Y., LIU, F., & Hao, Q. (2015). Characteristics of hydrogen and oxygen isotopes and renewal
986 of groundwater in the Nuomuhong alluvial fan. *Hydrogeology & Engineering Geology*, 42(6),
987 1-7 (in Chinese with English abstract).

988 Dansgaard, W. (1964). Stable isotopes in precipitation. *tellus*, 16(4), 436-468.

989 Durack, PJ, Wijffels, SE, & Matear, RJ (2012). Ocean salinities reveal strong global water cycle
990 intensification during 1950 to 2000. *Science*, 336(6080), 455-458.

991 [Juan, G., Li, Z., Qi, F., Ruifeng, Y., Tingting, N., Baijuan, Z., ... & Pengfei, L. \(2020\).](#)
992 [Environmental effect and spatiotemporal pattern of stable isotopes in precipitation on the](#)
993 [transition zone between the Tibetan Plateau and arid region. Science of The Total](#)
994 [Environment, 749, 141559.](#)

995 Haddeland, I., Heinke, J., Biemans, H., Eisner, S., Flörke, M., Hanasaki, N., ... & Wisser, D. (2014).
996 Global water resources affected by human interventions and climate change. Proceedings of
997 the National Academy of Sciences, 111(9), 3251-3256.

998 [He, Y., Zhao, C., Liu, Z., Wang, H., Liu, W., Yu, Z., ... & Ito, E. \(2016\). Holocene climate controls](#)
999 [on water isotopic variations on the northeastern Tibetan Plateau. Chemical Geology, 440,](#)
1000 [239-247.](#)

1001 Hooper, RP (2003). Diagnostic tools for mixing models of stream water chemistry. Water
1002 Resources Research, 39(3), 1055.

1003 Hooper, RP, Christophersen, N., & Peters, NE (1990). Modeling streamwater chemistry as a
1004 mixture of soilwater end-members—An application to the Panola Mountain catchment,
1005 Georgia, USA. Journal of Hydrology, 116(1-4), 321-343.

1006 Huntington, TG (2006). Evidence for intensification of the global water cycle: review and
1007 synthesis. Journal of Hydrology, 319(1-4), 83-95.

1008 Jasechko, S., Birks, SJ, Gleeson, T., Wada, Y., Fawcett, PJ, Sharp, ZD, ... & Welker, JM (2014).
1009 The pronounced seasonality of global groundwater recharge. Water Resources Research,
1010 50(11), 8845-8867.

1011 [Jasechko, S., Perrone, D., Befus, K. M., Bayani Cardenas, M., Ferguson, G., Gleeson, T., ... &](#)
1012 [Kirchner, J. W. \(2017\). Global aquifers dominated by fossil groundwaters but wells](#)
1013 [vulnerable to modern contamination. Nature Geoscience, 10\(6\), 425-429.](#)

1014 ~~[Jian, X., Weislogel, A., Pullen, A., & Shang, F. \(2020\). Formation and evolution of the Eastern](#)~~
1015 ~~[Kunlun Range, northern Tibet: Evidence from detrital zircon U-Pb geochronology and Hf](#)~~
1016 ~~[isotopes. Gondwana Research, 83, 63-79.](#)~~

1017 Jiao, JJ, Zhang, X., Liu, Y., & Kuang, X. (2015). Increased water storage in the Qaidam Basin, the
1018 North Tibet Plateau from GRACE gravity data. PloS one, 10(10), e0141442.

1019 Juan, G., Li, Z., Qi, F., Ruifeng, Y., Tingting, N., Baijuan, Z., ... & Pengfei, L. (2020).
1020 Environmental effect and spatiotemporal pattern of stable isotopes in precipitation on the

1021 transition zone between the Tibetan Plateau and arid region. *Science of The Total*
1022 *Environment*, 749, 141559.

1023 Kang, S., Cong, Z., Wang, X., Zhang, Q., Ji, Z., Zhang, Y., & Xu, B. (2019). The transboundary
1024 transport of air pollutants and their environmental impacts on Tibetan Plateau. *Chinese*
1025 *Science Bulletin*, 64(27), 2876-2884.

1026 Ke, L., Song, C., Wang, J., Sheng, Y., Ding, X., Yong, B., ... & Luo, S. (2022). Constraining the
1027 contribution of glacier mass balance to the Tibetan lake growth in the early 21st century.
1028 *Remote Sensing of Environment*, 268, 112779.

1029 Kong, Y., Wang, K., Pu, T., & Shi, X. (2019). Nonmonsoon precipitation dominates groundwater
1030 recharge beneath a monsoon-affected glacier in Tibetan Plateau. *Journal of Geophysical*
1031 *Research: Atmospheres*, 124(20), 10913-10930.

1032 Kuang, X., & Jiao, JJ (2016). Review on climate change on the Tibetan Plateau during the last half
1033 century. *Journal of Geophysical Research: Atmospheres*, 121(8), 3979-4007.

1034 Li, L., & Garzzone, CN (2017). Spatial distribution and controlling factors of stable isotopes in
1035 meteoric waters on the Tibetan Plateau: Implications for paleoelevation reconstruction. *Earth*
1036 *and Planetary Science Letters*, 460, 302-314.

1037 Li, L., Shen, H., Li, H., & Xiao, J. (2015). Regional differences of climate change in Qaidam Basin
1038 and its contributing factors. *Journal of Natural Resources*, 30, 641-650 (in Chinese with
1039 English abstract).

1040 Liu, F., Cui, Y., Zhang, G., Geng, F., & Liu, J. (2014). Using the ^3H and ^{14}C dating methods to
1041 calculate the groundwater age in Nuomuhong, Qaidam Basin. *Geoscience*, 28 (6), 1322-1328
1042 (in Chinese with English abstract).

1043 Liu, J., Song, X., Sun, X., Yuan, G., Liu, X., & Wang, S. (2009). Isotopic composition of
1044 precipitation over Arid Northwestern China and its implications for the water vapor origin-
1045 *Journal of Geographical Sciences*, 19(2), 164-174 (in Chinese with English abstract).

1046 [Ma, J., Ding, Z., Edmunds, W. M., Gates, J. B., & Huang, T. \(2009\). Limits to recharge of](#)
1047 [groundwater from Tibetan plateau to the Gobi desert, implications for water management in](#)
1048 [the mountain front. *Journal of Hydrology*, 364\(1-2\), 128-141.](#)

1049 Malard, A., Sinreich, M., & Jeannin, PY (2016). A novel approach for estimating karst
1050 groundwater recharge in mountainous regions and its application in Switzerland.
1051 *Hydrological Processes*, 30(13), 2153-2166.

1052 Masson-Delmotte, V., Zhai, P., Pirani, A., Connors, SL, Péan, C., Berger, S., ... & Zhou, B. (2021).
1053 Climate change 2021: the physical science basis. Contribution of working group I to the sixth
1054 assessment report of the intergovernmental panel on climate change, 2.

1055 Moran, BJ, Boutt, DF, & Munk, LA (2019). Stable and radioisotope systematics reveal fossil water
1056 as fundamental characteristic of arid orogenic-scale groundwater systems. *Water Resources*
1057 *Research*, 55(12), 11295-11315.

1058 Parnell, AC, Inger, R., Bearhop, S., & Jackson, AL (2010). Source partitioning using stable
1059 isotopes: coping with too much variation. *PloS one*, 5(3), e9672.

1060 [Rodriguez, N. B., Pfister, L., Zehe, E., & Klaus, J. \(2021\). A comparison of catchment travel times](#)
1061 [and storage deduced from deuterium and tritium tracers using StorAge Selection functions.](#)
1062 [Hydrology and Earth System Sciences, 25\(1\), 401-428.](#)

1063 Shen, C., Jia, L., & Ren, S. (2022). Inter-and Intra-Annual Glacier Elevation Change in High
1064 Mountain Asia Region Based on ICESat-1&2 Data Using Elevation-Aspect Bin Analysis
1065 Method. *Remote Sensing*, 14(7), 1630.

1066 Shi, D., Tan, H., Chen, X., Rao, W., & Basang, R. (2021). Uncovering the mechanisms of seasonal
1067 river-groundwater circulation using isotopes and water chemistry in the middle reaches of
1068 the Yarlungzangbo River, Tibet. *Journal of Hydrology*, 603, 127010.

1069 Song, C., Huang, B., Richards, K., Ke, L., & Hien Phan, V. (2014). Accelerated lake expansion
1070 on the Tibetan Plateau in the 2000s: Induced by glacial melting or other processes?. *Water*
1071 *Resources Research*, 50(4), 3170-3186.

1072 [Stewart, M. K., Morgenstern, U., Gusyev, M. A., & Małoszewski, P. \(2017\). Aggregation effects](#)
1073 [on tritium-based mean transit times and young water fractions in spatially heterogeneous](#)
1074 [catchments and groundwater systems. Hydrology and Earth System Sciences, 21\(9\), 4615-](#)
1075 [4627.](#)

1076 [Tan, H., Chen, J., Rao, W., Zhang, W., & Zhou, H. \(2012\). Geothermal constraints on enrichment](#)
1077 [of boron and lithium in salt lakes: An example from a river-salt lake system on the northern](#)
1078 [slope of the eastern Kunlun Mountains, China. Journal of Asian Earth Sciences, 51, 21-29.](#)

1079 [Tan, H., Rao, W., Chen, J., Su, Z., Sun, X., & Liu, X. \(2009\). Chemical and isotopic approach to](#)
1080 [groundwater cycle in western Qaidam Basin, China. Chinese Geographical Science, 19, 357-](#)
1081 [364.](#)

- 1082 Tan, H., Zhang, Y., Rao, W., Guo, H., Ta, W., Lu, S., & Cong, P. (2021). Rapid groundwater
1083 circulation inferred from temporal water dynamics and isotopes in an arid system.
1084 *Hydrological Processes*, 35(6), e14225.
- 1085 Tian, L., Yao, T., Sun, W., Stievenard, M., & Jouzel, J. (2001). Relationship between δD and $\delta^{18}O$
1086 in precipitation on north and south of the Tibetan Plateau and moisture recycling. *Science in*
1087 *China Series D: Earth Sciences*, 44(9), 789-796.
- 1088 Wang, L., Yao, T., Chai, C., Cuo, L., Su, F., Zhang, F., Yao, Z., Zhang, Y., Li, X., Qi, J., Hu, Z.,
1089 Liu, J., & Wang, Y. (2021). TP-River: Monitoring and Quantifying Total River Runoff from
1090 the Third Pole, *Bulletin of the American Meteorological Society*, 102(5), E948-E965.
- 1091 Wang, S., Lei, S., Zhang, M., Hughes, C., Crawford, J., Liu, Z., & Qu, D. (2022). Spatial and
1092 seasonal isotope variability in precipitation across China: Monthly isoscapes based on
1093 regionalized fuzzy clustering. *Journal of Climate*, 35(11), 3411-3425.
- 1094 [Wang, S., Zhang, M., Che, Y., Chen, F., & Qiang, F. \(2016\). Contribution of recycled moisture to](#)
1095 [precipitation in oases of arid central Asia: A stable isotope approach. *Water Resources*](#)
1096 [Research, 52\(4\), 3246-3257.](#)
- 1097 [Wang, T., Yang, D., Yang, Y., Zheng, G., Jin, H., Li, X., ... & Cheng, G. \(2023\). Unsustainable](#)
1098 [water supply from thawing permafrost on the Tibetan Plateau in a changing climate. *Science*](#)
1099 [bulletin, S2095-9273.](#)
- 1100 Wang, X., Chen, M., Gong, P., & Wang, C. (2019). Perfluorinated alkyl substances in snow as an
1101 atmospheric tracer for tracking the interactions between westerly winds and the Indian
1102 Monsoon over western China. *Environment international*, 124, 294-301.
- 1103 Wang, X., Yang, M., Liang, X., Pang, G., Wan, G., Chen, X., & Luo, X. (2014). The dramatic
1104 climate warming in the Qaidam Basin, northeastern Tibet Plateau, during 1961–2010.
1105 *International Journal of Climatology*, 34(5), 1524-1537.
- 1106 Wang, Y., Guo, H., Li, J., Huang, Y., Liu, Z., Liu, C., Guo, X., Zhou, J., Shang, X., Li, J., Zhuang,
1107 Y., & Cheng, H. (2008). Investigation and assessment of groundwater resources and their
1108 environmental issues in the Qaidam Basin. Geological Publishing House, [Beijing \(in Chinese\)](#).
- 1109 Wei, L., Jiang, S., Ren, L., Tan, H., Ta, W., Liu, Y., ... & Duan, Z. (2021). Spatiotemporal changes
1110 of terrestrial water storage and possible causes in the closed Qaidam Basin, China using
1111 GRACE and GRACE Follow-On data. *Journal of Hydrology*, 598, 126274.

- 1112 [Wen, G., Wang, W., Duan, L., Gu, X., Li, Y., & Zhao, J. \(2018\). Quantitatively evaluating](#)
1113 [exchanging relationship between river water and groundwater in Bayin River Basin of](#)
1114 [northwest China using hydrochemistry and stable isotope. *Arid Land Geography*, 41, 734-](#)
1115 [743 \(in Chinese with English abstract\).](#)
- 1116 Wu, H., Zhang, C., Li, XY, Fu, C., Wu, H., Wang, P., & Liu, J. (2022). Hydrometeorological
1117 Processes and Moisture Sources in the Northeastern Tibetan Plateau: Insights from a 7-Yr
1118 Study on Precipitation Isotopes. *Journal of Climate*, 35(20), 2919-2931.
- 1119 Xiang, L., Wang, H., Steffen, H., Wu, P., Jia, L., Jiang, L., & Shen, Q. (2016). Groundwater storage
1120 changes in the Tibetan Plateau and adjacent areas revealed from GRACE satellite gravity data.
1121 *Earth and Planetary Science Letters*, 449, 228-239.
- 1122 Xiao, Y., Shao, J., Cui, Y., Zhang, G., & Zhang, Q. (2017). Groundwater circulation and
1123 hydrogeochemical evolution in Nomhon of Qaidam Basin, northwest China. *Journal of Earth*
1124 *System Science*, 126 (2), 1-16.
- 1125 Xiao, Y., Shao, J., Frapce, SK, Cui, Y., Dang, X., Wang, S., & Ji, Y. (2018). Groundwater origin,
1126 flow regime and geochemical evolution in arid endorheic watersheds: a case study from the
1127 Qaidam Basin, northwestern China. *Hydrology and Earth System Sciences*, 22(8), 4381-4400.
- 1128 Xu, W., Su, X., Dai, Z., Yang, F., Zhu, P., & Huang, Y. (2017). Multi-tracer investigation of river
1129 and groundwater interactions: a case study in Nalenggele River basin, northwest China.
1130 *Hydrogeology Journal*, 25(7), 2015-2029.
- 1131 Yang, N., & Wang, G. (2020). Moisture sources and climate evolution during the last 30 kyr in
1132 northeastern Tibetan Plateau: Insights from groundwater isotopes (2H, 18O, 3H and 14C) and
1133 water vapor trajectories modeling. *Quaternary Science Reviews*, 242, 106426.
- 1134 Yang, N., Wang, G., Liao, F., Dang, X., & Gu, X. (2023). Insights into moisture sources and
1135 evolution from groundwater isotopes (2H, 18O, and 14C) in Northeastern Qaidam Basin,
1136 Northeast Tibetan Plateau, China. *Science of The Total Environment*, 864, 160981.
- 1137 Yang, N., Zhou, P., Wang, G., Zhang, B., Shi, Z., Liao, F., ... & Gu, X. (2021). Hydrochemical
1138 and isotopic interpretation of interactions between surfaces water and groundwater in
1139 Delingha, Northwest China. *Journal of Hydrology*, 598, 126243.
- 1140 Yang, Y., Wu, Q., & Jin, H. (2016). Evolutions of water stable isotopes and the contributions of
1141 cryosphere to the alpine river on the Tibetan Plateau. *Environmental Earth Sciences*, 75(1),
1142 1-11-.

- 1143 Yao, T., Bolch, T., Chen, D., Gao, J., Immerzeel, W., Piao, S., ... & Zhao, P. (2022). The imbalance
1144 of the Asian water tower. *Nature Reviews Earth & Environment*, 1-15.
- 1145 Yao, T., Masson-Delmotte, V., Gao, J., Yu, W., Yang, X., Risi, C., ... & Hou, S. (2013). A review
1146 of climatic controls on $\delta^{18}\text{O}$ in precipitation over the Tibetan Plateau: Observations and
1147 simulations. *Reviews of Geophysics*, 51(4), 525-548.
- 1148 [Ye, C., Zheng, M., Wang, Z., Hao, W., Wang, J., Lin, X., & Han, J. \(2015\). Hydrochemical
1149 characteristics and sources of brines in the Gasikule salt lake, Northwest Qaidam Basin, China.
1150 *Geochemical Journal*, 49\(5\), 481-494.](#)
- 1151 Zhang, G., Yao, T., Shum, CK, Yi, S., Yang, K., Xie, H., ... & Yu, J. (2017). Lake volume and
1152 groundwater storage variations in Tibetan Plateau's endorheic basin. *Geophysical Research
1153 Letters*, 44(11), 5550-5560.
- 1154 Zhang, Q., Zhu, B., Yang, J., Ma, P., Liu, X., Lu, G., ... & Wang, D. (2021). New characteristics
1155 about the climate humidity trend in Northwest China. *Chinese Science Bulletin*, 66, 3757-
1156 3771.
- 1157 Zhang, X., Chen, J., Chen, J., Ma, F., & Wang, T. (2022). Lake Expansion under the Groundwater
1158 Contribution in Qaidam Basin, China. *Remote Sensing*, 14(7), 1756 .
- 1159 Zhao, D., Wang, G., Liao, F., Yang, N., Jiang, W., Guo, L., ... & Shi, Z. (2018). Groundwater-
1160 surface water interactions derived by hydrochemical and isotopic (^{222}Rn , deuterium,
1161 oxygen-18) tracers in the Nomhon area, Qaidam Basin, NW China. *Journal of Hydrology*,
1162 565, 650-661.
- 1163 Zhao, D., Wang, G., Liao, F., Yang, N., Jiang, W., Guo, L., ... & Shi, Z. (2018). Groundwater-
1164 surface water interactions derived by hydrochemical and isotopic (^{222}Rn , deuterium,
1165 oxygen-18) tracers in the Nomhon area, Qaidam Basin, NW China. *Journal of Hydrology*,
1166 565, 650-661.
- 1167 Zhao, L., Yin, L., Xiao, H., Cheng, G., Zhou, M., Yang, Y., ... & Zhou, J. (2011). of surface runoff
1168 in the headwaters of the Heihe River basin. *Chinese Science Bulletin*, 56(4), 406-415.
- 1169 [Zhu, G., Liu, Y., Wang, L., Sang, L., Zhao, K., Zhang, Z., ... & Qiu, D. \(2023\). The isotopes of
1170 precipitation have climate change signal in arid Central Asia. *Global and Planetary Change*,
1171 225, 104103.](#)

1172 Zhu, J., Chen, H., & Gong, G. (2015). Hydrogen and oxygen isotopic compositions of precipitation
1173 and its water vapor sources in Eastern Qaidam Basin. *Environmental Science*, 36(8), 2784-
1174 2790 (in Chinese with English abstract).

1175 [Zhu, P. \(2015\). Groundwater circulation patterns of Yuqia-Maihai Basin in the middle and lower](#)
1176 [reaches of Yuqia River. Doctoral dissertation, Jilin University, Changchun \(in Chinese with](#)
1177 [English abstract\).](#)

1178 Zou, Y., Kuang, X., Feng, Y., Jiao, JJ, Liu, J., Wang, C., ... & Zheng, C. (2022). Solid water melt
1179 dominates the increase of total groundwater storage in the Tibetan Plateau. *Geophysical*
1180 *Research Letters*, e2022GL100092.

1181